phosphorylation, whereby it translocates to the nucleus to act as a transcriptional factor for positive regulatory domain (PRD) I of the IFN-β promoter. IRF-3 activation also induces phosphorylation of Ser385 and Ser386 or the serine/threonine (Ser/Thr) cluster between amino acids (aa) 396 and 405 (located at the C-terminus of IRF-3), a step that is essential for dimerization and nuclear translocation.

A previous study by Foy et al. showed that the NS3/4A serine protease derived from a subgenomic replicon participates in the suppression of the cellular pathway that activates IRF-3 [12]. The NS3/4A protein of HCV disrupts signaling of the double-stranded RNA (dsRNA) receptors, retinoic acid-inducible gene-I (RIG-I), and Toll-like receptor 3 (TLR3) by inducing proteolysis of interferon promoter stimulator-1 (IPS-1) [13–15] and Toll/interleukin-1 receptor (TIR) domain-containing adaptor protein inducing IFN-β (TRIF) [16], as well as by suppressing the downstream activation of IFN-β [13].

In view of the above observations and the emerging data on the role of HCV in regulating the IRF-3 pathway by additional mechanisms, we aimed to investigate the effects of various HCV proteins on IRF-3 activation, and further elucidate the underlying novel mechanisms.

2. Material and methods

2.1. Transient expression of the HCV core proteins E1, E2, and NS3-4A

HepG2 cells were transfected to express E1, E2, or NS3-4A HCV core protein under the control of EF promoter (Invitrogen). The HCV core expression vectors were derived from HCR6 (genotype 1b), HCR24-12K (genotype 2a), or HCR24-12Q (genotype 2a). The E1, E2, and NS3 clones derived from HCR6 contained either the full-length cDNAs encoding the core protein or 1 of the 3 different deletions (deletion mutants), each of which lacked 1 of the 3 basic amino acid regions (BR), BR1 deletion (aa 4–14), BR2 deletion (aa 37–44), and BR3 deletion (aa 57–72) [17]. HepG2 cells were transfected with 4 μg of the core cDNA (amino acids 1–191), E1 (amino

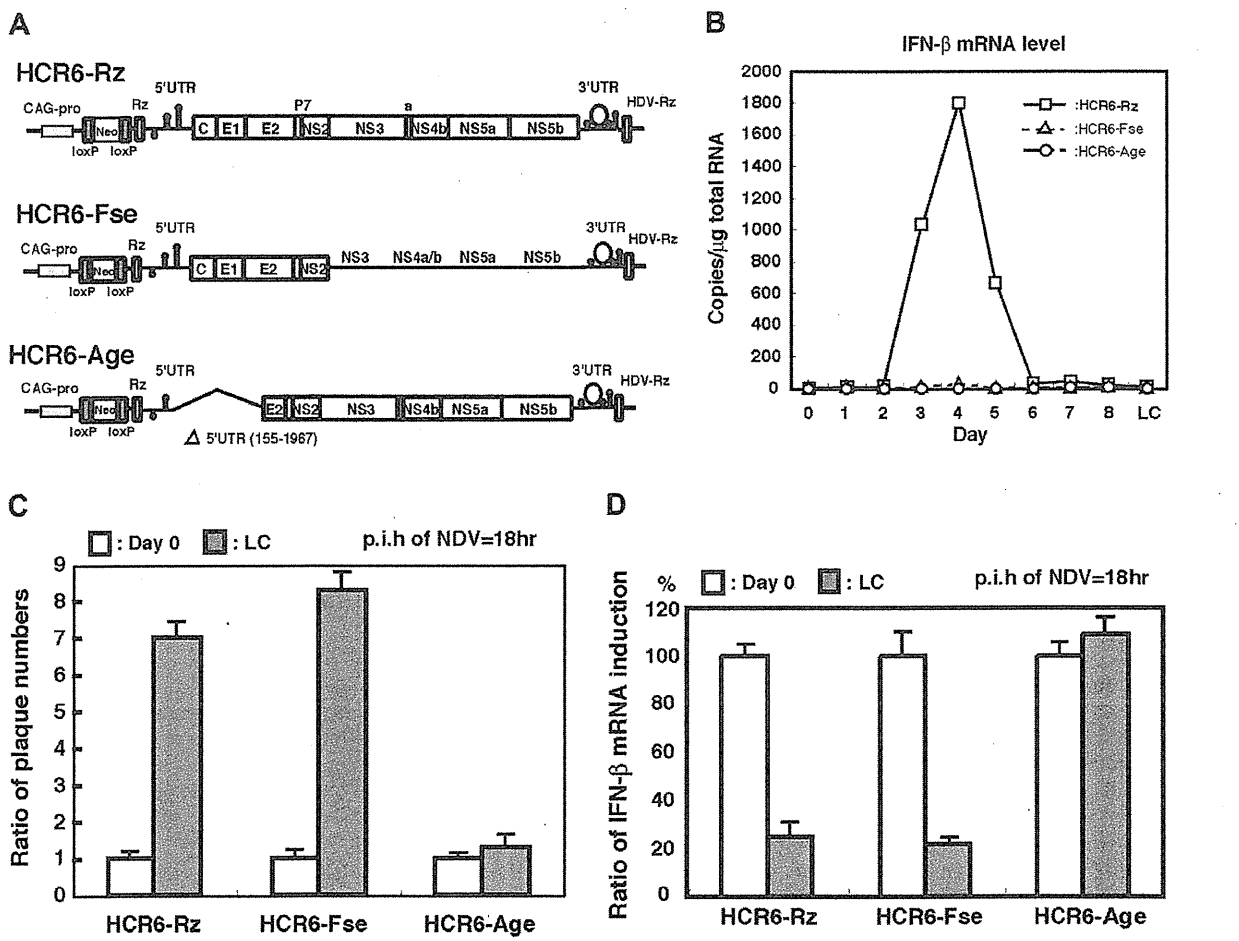

Fig. 1. (A) Structures of the conditional expression vectors for HCV RNAs and proteins. The cDNA clones that displayed highest level of homology to the consensus sequences among the 3 clones were used to construct *HCR6-Rz* (nt 1–9611). *HCR6-Fse* clone harbored a termination codon introduced at nucleotide 3606 and truncated *HCR6-Age* clone lacked nucleotides 155–1967. They were flanked with ribozyme (Rz) and hepatitis D virus ribozyme (HDV-Rz) sequences under the control of the CAG promoter in the Cre/*loxP* switching expression cassette, which consisted of the neomycin resistance gene, as a stuffer region flanked by the *loxP* sequence. (B) IFN-β mRNA levels in the cell lines *HCR6-Rz*, *HCR6-Fse*, and *HCR6-Age* before and after the expression of the HCV protein. The results are expressed as copy numbers per microgram of total RNA, as quantified by RT-PCR. (C) Efficiency of NDV plaque formation. Plaque assays were performed on Vero cells for NDV infectivity in *HCR6-Rz*, *HCR6-Fse*, or *HCR6-Age* before and after the expression of the HCV protein. The plaque numbers were counted 3 days after NDV inoculation. The ratio indicates the plaque numbers after the expression of the HCV genome divided by the plaque numbers before the expression of the HCV genome. (D) Suppression of IFN-β mRNA induction by HCV expression, 18 days after NDV inoculation. Day 0, before the expression of the HCV genome; Day 48, after the expression of the HCV genome. The results are expressed relative to the levels on Day 0 (100%) in each of the 3 HCV-expressing systems. p.i.h., post-inoculation hour.

acids 192–383), E2 (amino acids 384–809), NS3-4A (amino acids 1027–1711), or the core regions lacking the BR, in 35-mm dishes, by using Lipofectamine 2000 (Invitrogen) at 37 °C for 6 h. The medium was subsequently replaced with normal culture medium, and the cells were harvested after 48 h.

2.2. Newcastle disease virus (NDV) infection and addition of polyriboinosinic:polyribocytidylic acid [poly(I:C)]

NDV (Miyadera strain) was propagated from swabs by using the embryonated egg culture method, as described in the Supplementary methods.

Poly(I:C) (20 μg/well; GE Healthcare) was added to HepG2 cells in 35-mm dishes, 48 h after transfection with the core expression vector derived from HCR6 (genotype 1b).

2.3. Native PAGE of IRF-3 and phosphorylated IRF-3

Cells were lysed in 30 μL of lysis buffer (50 mM Tris–HCl [pH 8.0], 1% NP-40, 150 mM NaCl, 100 μg/mL leupeptin, 1 mM PMSF, 5 mM Na_3VO_4), mixed vigorously, and centrifuged at 15,000 rpm for 10 min; the supernatant was isolated. Total protein samples (10 μg) were electrophoresed on a 7.5% native PAGE gel (Bio-Rad Laboratories) and transferred onto a PVDF membrane. IRF-3 homodimer and its monomer and Ser386-phosphorylated IRF-3 were detected by western blotting using polyclonal rabbit antibodies, anti-human IRF-3 (1:1000) [18] and, anti-human Ser386-phosphorylated IRF-3 (1:10,000), respectively. Detection was achieved by enhanced chemiluminescence (ECL; Amersham, UK) according to the manufacturer's instructions. The rabbit anti-human IRF-3 and anti-human Ser386-phosphorylated IRF-3 antibodies were described previously [19].

2.4. Quantification of IFN-β gene expression

IFN-β mRNA expression was quantified by using real-time PCR (RT-PCR) as described previously [20] and Supplementary methods using the following primers and probes: sense (5′-CCATCTATGA GATGCTCCAGAA-3′), antisense (5′-TTTTCTTCCAGGACTGTCTTCA-GA-3′) and probe (5′-AGCACTGGCTGGAATGAGACTATTGTTG-3′).

3. Results

3.1. Induction of IFN and IRF-3 by HCV-Rz

To evaluate the effect of HCV gene persistent expression, cell lines expressing the HCV genomes in a Cre/*lox*P expression system [20] were established by transfecting the full-genome HCV (*HCR6-Rz*); core, E1, E2, and NS2 (*HCR6-Fse*); and E2~NS5b (*HCR6-Age*) (Fig. 1A) clones into HepG2 cells. Of the 3 HCV expression systems, only *HCR6-Rz* transiently induced endogenous IFN-β expression (Fig. 1B). No endogenous IFN-β was detected by RT-PCR on Day 0 or Day 48 (long culture; LC) [21] in any of the 3 systems (Fig. 1B).

3.2. Effect of HCV expression on NDV infection and IFN-β induction

Further, we examined whether the persistent expression of HCV genome influenced the plaque formation activity of NDV in *HCR6-Rz*-, *HCR6-Fse*-, and *HCR6-Age*-expressing cell lines. Prior to the expression of HCV proteins, the plaque numbers were similar across all the cell lines (Fig. 1C). Expression of HCV proteins for more than 48 days [21] increased plaque numbers in the *HCR6-Rz*- and *HCR6-Fse*-expressing cells from 7- to 8-fold (Fig. 1C); however, plaque numbers in the *HCR6-Age*-expressing cells remained constant. These findings thus indicate that HCV structural proteins interfered with the induction of IFN-β mRNA, after NDV infection (18 h post-infection). Therefore, we measured IFN-β mRNA levels in the 3 cell lines, *HCR6-Rz*, *HCR6-Fse*, and *HCR6-Age*, by RT-PCR before (Day 0) and after (Day 48) inoculation with NDV (Fig. 1D). The mRNA expression of IFN-β was not observed prior to NDV infection in any of the 3 cell lines (Day 0). Notably, after 18 h of NDV inoculation and prior to the expression of various HCV proteins (Day 0), the levels of IFN-β mRNA transcription were similar among *HCR6-Rz*-, *HCR6-Fse*-, and *HCR6-Age*-expressing cell lines (Fig. 1D). Following HCV protein expression, the induced IFN-β mRNA expression was reduced to 20% in both *HCR6-Rz*- and *HCR6-Fse*-expressing cell lines. However, IFN-β mRNA expression remained constant in the *HCR6-Age*-expressing cell line.

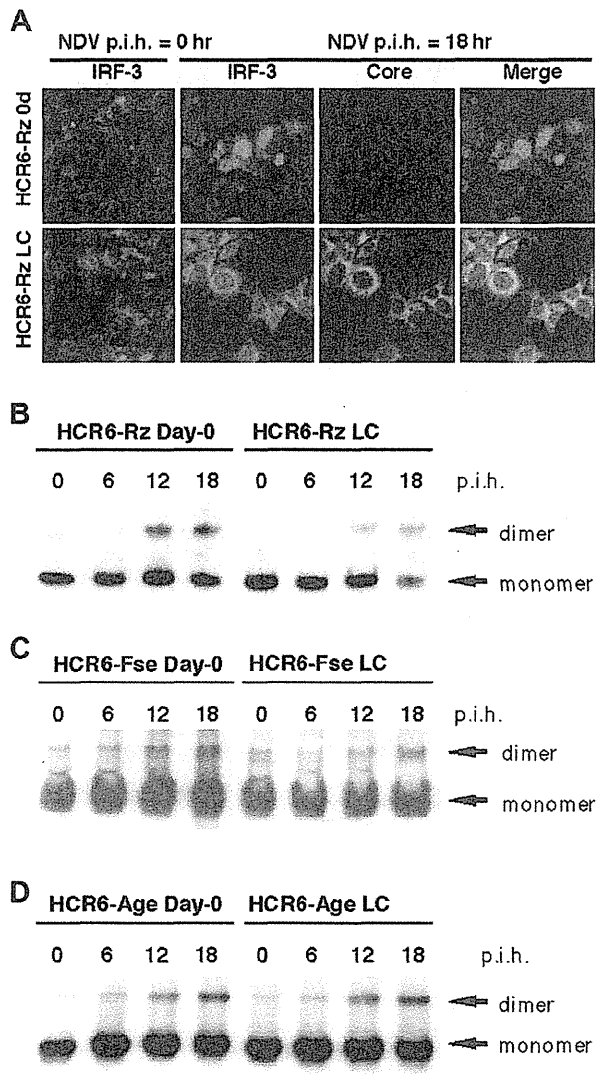

Fig. 2. (A) HCV inhibition of IRF-3 nuclear translocation. IRF-3 is a constitutively expressed transcriptional factor that localizes in the cytoplasm in a diffuse manner, when inactive. After NDV inoculation and prior to the expression of the HCV genome, IRF-3 translocated to the nucleus but was retained at a perinuclear site in the *HCR6-Rz*-expressing cells (Day 48). IRF-3 colocalized with the HCV core protein. (B–D) Suppression of IRF-3 dimerization by HCV expression. The dimeric and monomeric forms of IRF-3 were detected by western blotting on native PAGE gels. The influence of (B) *HCR6-Rz* expression, (C) *HCR6-Fse* expression, and (D) *HCR6-Age* expression on IRF-3 dimerization is shown. NDV was used to induce IRF-3 dimerization.

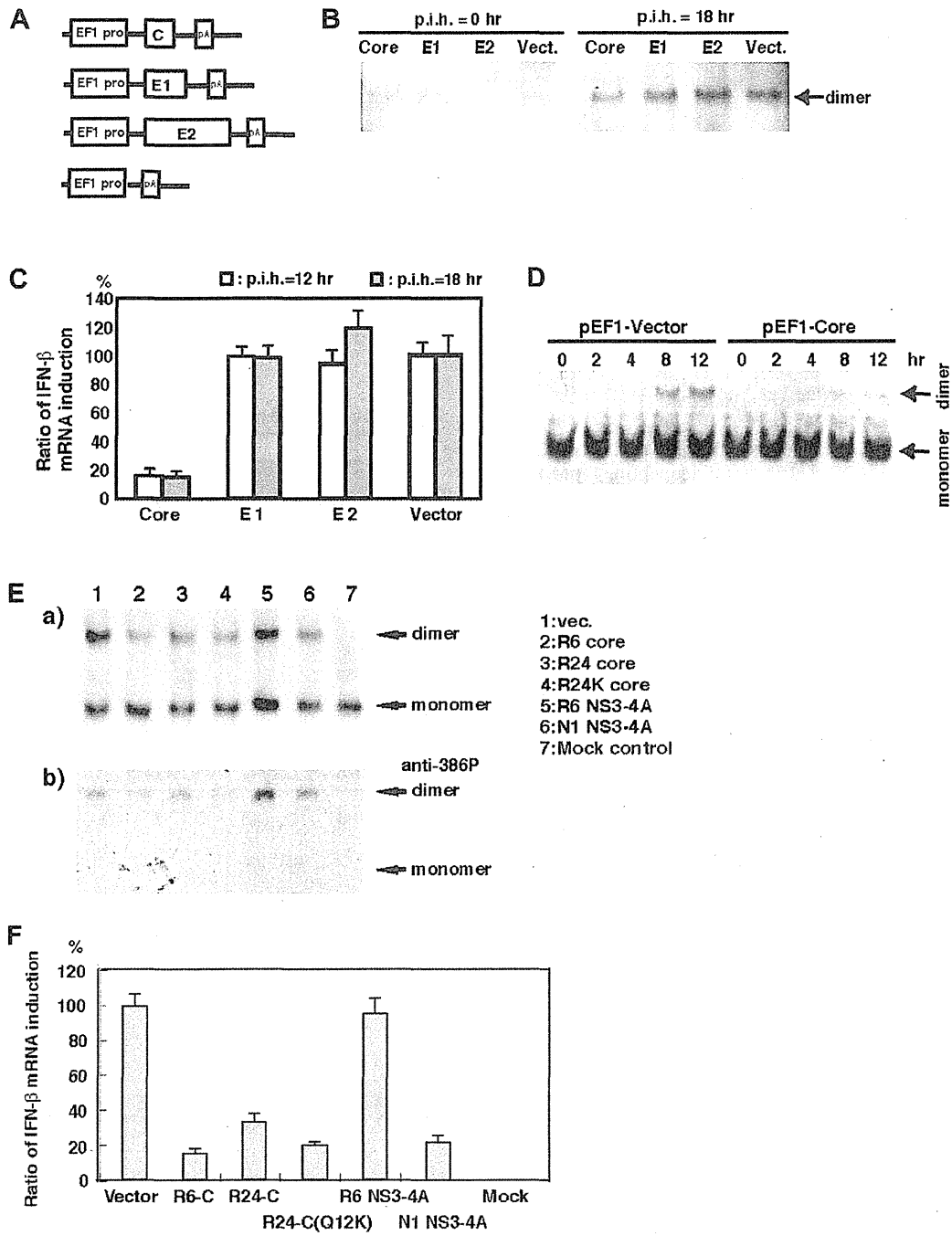

Fig. 3. (A) Structures of the HCR6 core, E1, and E2 expression vectors encoding the HCV core (aa 1–191), E1 (amino acids 192–383), and E2 (amino acids 384–809) proteins, respectively, under the control of the EF1 promoter. (B) Left panel, IRF-3 dimerization induced by NDV before transfection with the expression vectors; right panel, IRF-3 dimerization induced by NDV after transfection with the expression vectors. (C) IFN-β mRNA induction levels at 12 and 18 h after NDV inoculation into HepG2 cells transfected with the vector alone, core, E1, or E2 proteins. The results are expressed relative to the induction levels of IFN-β in HepG2 cells transfected with the vector alone (100%), for post-inoculation, each time. (D) IRF-3 dimerization on administration of 10 mg/mL poly(I:C) before the expression (Day 0), and at 2, 4, 8, and 12 h after the expression of the HCV core (pEF-Core) or vector plasmid DNA. (E) Effects of the expression of vector (lane 1), R6 core (lane 2), R24 core (lane 3), R24 core (Q12K) (lane 4), R6-NS3-4A (lane 5), N1-NS3-4A (lane 6), and mock control (lane 7) on IRF-3 dimerization (upper column a) and phosphorylation of serine residue at amino acid 386 in IRF-3 (lower column b), after infection with NDV for 18 h. F. Effects of the expressions of R6-C, R24-C, R24-C(Q12K), and R6-NS3 on IFN-β induction, 18 h after NDV inoculation. The IFN-β mRNA levels were assayed by RT-PCR. The results are expressed relative to the induction levels of IFN-β in HepG2 cells transfected with the vector alone (100%).

3.3. Effect of HCV on IRF-3 localization, nuclear translocation, and dimerization by NDV

The effect of HCV expression on cellular localization of IRF-3 was analyzed in *HCR6-Rz*-expressing cells infected with NDV before (Day 0) and after LC (Fig. 2A). Prior to NDV infection, IRF-3 was detected in the cytoplasm by immunofluorescence. Notably, after 18 h of NDV inoculation and prior to *HCR6-Rz* protein expression, when IFN-β induction and IRF-3 dimerization were maximal, a substantial amount of IRF-3 translocated to the nucleus.

However, this nuclear translocation was suppressed in the presence of HCV proteins (Fig. 2A) and resulted in the co-localization of the HCV core protein with IRF-3 at perinuclear sites (Fig. 2A, superimposed image of IRF-3 and core protein immunostaining).

To elucidate the mechanism underlying the suppression of IFN-β mRNA in *HCR6-Rz*- and *HCR6-Fse*-expressing cells, we examined the effect of HCV expression on IRF-3 dimerization after NDV infection (Fig. 2B). Interestingly, the levels of IRF-3 dimerization peaked at 12–18 h after NDV infection in the 3 cell lines lacking HCV expression (Day 0; Fig. 2). However, in the *HCR6-Rz*- and *HCR6-Fse*-expressing cell lines, IRF-3 dimerization was found to be significantly reduced, (Fig. 2B and C) when compared to that in the *HCR6-Age*-expressing cells (Fig. 2D).

3.4. Identification of the HCV genome region responsible for the inhibition of IRF-3 dimerization and IFN-β induction

To identify the HCV genome region responsible for suppression of IRF-3 dimerization, HepG2 cells were transfected to express the HCV core regions derived from HCR6, E1, or E2 (genotype 1b; Fig. 3A). Protein expression was confirmed by western blotting (data not shown). The HCV core protein suppressed IRF-3 dimerization, but E1 and E2 expressions had no effect on the dimerization (Fig. 3B). Expression of E1, E2, or the vector alone did not alter the levels of IFN-β mRNA induced by NDV infection in HepG2 cells (Fig. 3C), but significantly reduced IFN-β mRNA levels at both 12 and 18 h after infection (Fig. 3C).

3.5. Effect of HCV core protein expression on IRF-3 dimerization through TLR3

Among the synthetic dsRNAs, poly(I:C) is a potent inducer of IFN-β through TLR3. Accordingly, HepG2 cells transfected with poly(I:C) and the vector control (pEF1-vector) showed IRF-3 dimerization (Fig. 3D). In contrast, IRF-3 dimerization was suppressed in HepG2 cells expressing the HCV core protein albeit the induction of IFN-β mRNA following poly(I:C) expression (data not shown).

3.6. Effect of the HCV core protein NS3 and core proteins derived from genotype 2a on IRF-3 dimerization, compared to proteins derived from genotype 1b

Further, we investigated whether the HCV core protein NS3 and core proteins derived from other genotypes exerted the same effects on IRF-3 after 18 h of NDV infection. The core proteins derived from genotypes 1b (R6) and 2a (R24-12Q and R24-12K) suppressed IRF-3 dimerization in cells infected with NDV (Fig. 3E(a)). In contrast, IRF-3 dimerization remained unaltered in the presence of R6 clone NS3 protein, but was suppressed by the N clone NS3 protein. Thus, NS3-4A protein of R6 clone suppressed IRF-3 dimerization to a relatively lesser extent compared to that of the N1 strain. Similar results were obtained for the phosphorylation at Ser386 in IRF-3 (Fig. 3E(b)). The IFN-β mRNA transcription was quantified in HepG2 cells by RT-PCR after transfection with these expression vectors (Fig. 3F).

3.7. Identification of the HCV core region responsible for suppressing IRF-3 dimerization

We sought to identify the region of the HCV core protein responsible for suppressing IRF-3 dimerization. Expression vectors encoding the entire HCV core or the core region lacking 1 of the 3 basic amino acid regions (BR) that influenced nuclear translocation [17] were transfected into HepG2 cells, and the effects on IRF-3 dimerization were examined (Fig. 4A). Protein

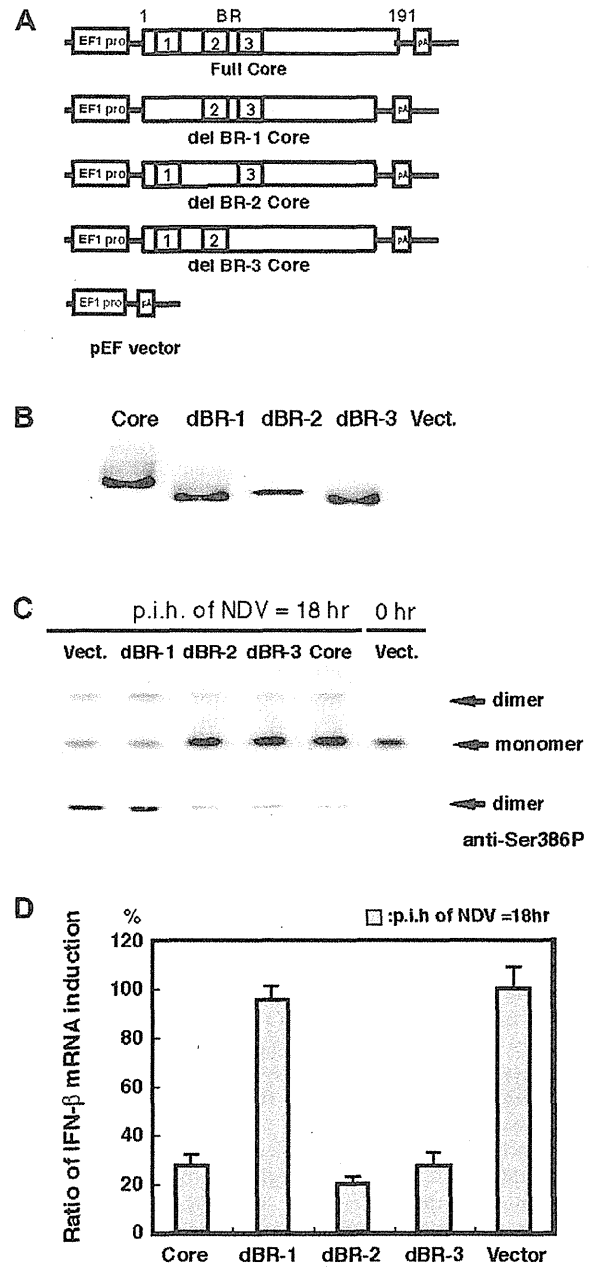

Fig. 4. (A) Structures of the HCR6 core, E1, and E2 expression vectors carrying the complete core, BR1 deletion (aa 4–14), BR2 deletion (aa 37–44), and BR3 deletion (aa 57–72). (B) Western blotting to confirmed the expression of the mutated core proteins. (C) Effects of the expression of various mutated core proteins on IRF-3 dimerization and IRF-3 phosphorylation at Ser386, 18 h after NDV inoculation. (D) Effects of the expression of each type of core protein region on IFN-β mRNA synthesis, 18 h after NDV inoculation. The results are expressed relative to the induction levels of IFN-β in HepG2 cells transfected with the vector alone (100%). IFN-β mRNA levels were assayed by RT-PCR.

expression of the core and the deletion mutants (BR1, BR2, and BR3) was confirmed by western blotting (Fig. 4B). IRF-3 dimerization, phosphorylation at Ser386 of IRF-3, and induction of IFN-β mRNA were suppressed in HepG2 cells expressing the entire core, a deletion of BR2, or a deletion of BR3 (Fig. 4C), but not in cells expressing the BR1-deleted HCV core regions (Fig. 4C and D).

4. Discussion

The present study indicates that the HCV core protein inhibits IRF-3 dimerization, IRF-3 phosphorylation at Ser386, and IFN-β induction. In addition, our study showed that the effect of the core protein derived from genotype 1b was similar to that of the core protein derived from genotype 2a, indicating that the inhibitory effect of the core protein might be effective in several genotypes of HCV. These findings are corroborated by a previous study by Foy et al. [12] who showed that HCV NS3/4 disrupts virus-associated-kinase-mediated IRF-3 activation, which further results in the suppression of IRF-3 phosphorylation, nuclear translocation, and IRF-3-dependent ISRE/PRDI activation. These findings indicate that attenuation of the IFN system was achieved through NS3/4A proteins via the interference of IRF-3 activation, thus strengthening our results, which show the potential of HCV core protein to interfere with IRF-3 activation in promoting persistent infection.

Furthermore, the present study showed that the N-terminal region of the core protein and BR-1 domain in particular are responsible for inactivating IRF-3. The N-terminal region (amino acids 1–59) of the HCV core protein has been identified as the binding region for a DEAD box protein (DDX3) [22]. Human DDX3, a putative RNA helicase, is a member of the highly conserved DEAD box subclass that includes the expression of murine PL10, *Xenopus* An3, and yeast Ded 1 proteins. Recently, expression of DDX3 was found to enhance IFN-β promoter induction by TBK1/IKKε, whereas silencing of DDX3 inhibited IFN-β promoter and virus- or dsRNA-induced IRF-3 activation [23]. It was shown that Vaccinia virus K7 protein also binds to DDX3 and inhibits pattern recognition receptor-induced IFN-β induction by preventing TBK1/IKKε-mediated IFN-β induction via impaired TBK1/IKKε-induced activation of IRF-3 [23]. A previous study by Oshiumi et al. showed that DDX3 C-terminal region (amino acids 622–662) directly binds to the IFN-beta promoter stimulator-1 (IPS-1) CARD-like domain [24] as well as the N-terminal HCV core protein [36]. The present study demonstrated that the expression of the core protein decreased the levels of DDX3 expression (data not shown). This is in agreement with the result of a previous study, which showed that DDX3 is downregulated in HCV-associated hepatocellular carcinoma (HCC) and silencing of DDX3 accelerates cell growth [25]. Collectively, these findings suggest that DDX3 may be the target of the core protein for inhibiting IRF-3 activation.

In conclusion, our study revealed a crucial region of the HCV core protein, basic amino acid region 1, to interfere with IRF-3 activation and thereby inhibit the IFN signaling cascades. Therefore, the inhibitory effects that result in the IRF-3 pathway impairment could be rescued by deleting the basic region 1 of core protein, thus suggesting that it might be an effective treatment for HCV infection. Future studies involving DDX3 modification by the HCV core protein may be interesting to explore the cell growth-dysregulation mechanisms.

Acknowledgments

This study was supported in part by a grant from the Ministry of Education, Culture, Sports, Science and Technology of Japan; a grant from the Ministry of Health, Labour and Welfare of Japan; and the Program for Promotion of Fundamental Studies in Health Sciences of the National Institute of Biomedical Innovation of Japan; and the Cooperative Research Project on Clinical and Epidemiological Studies of Emerging and Re-emerging Infectious Diseases.

Appendix A. Supplementary data

Supplementary data associated with this article can be found, in the online version, at http://dx.doi.org/10.1016/j.bbrc.2012.10.079.

References

[1] N. Kato, M. Hijikata, Y. Ootsuyama, et al., Molecular cloning of the human hepatitis C virus genome from Japanese patients with non-A, non-B hepatitis, Proc. Natl. Acad. Sci. USA 87 (1990) 9524–9528.
[2] L.B. Seeff, F.B. Hollinger, H.J. Alter, et al., Long-term mortality and morbidity of transfusion-associated non-A, non-B, and type C hepatitis: a National Heart, Lung, and Blood Institute collaborative study, Hepatology 33 (2001) 455–463.
[3] H.B. El-Serag, Hepatocellular carcinoma and hepatitis C in the United States, Hepatology 36 (2002) S74–S83.
[4] D. Thomas, The hepatitis C viruses, in: C. Hagedorn, C. Rice (Eds.), Hepatitis C Epidemiology, Springer-Verlag, Berlin, 1999, pp. 25–42.
[5] G.R. Foster, Interferons in host defense, Semin. Liver Dis. 17 (1997) 287–295.
[6] R. Kaufman, Translation control of genome expression, in: N Sonenberg, J Hershey, M Matthews (Eds.), The double strand RNA-activated protein kinase PKR, Cold Spring Harbor, New York, 2000, pp. 503–527.
[7] M.J. Gale Jr., M.J. Korth, N.M. Tang, et al., Evidence that hepatitis C virus resistance to interferon is mediated through repression of the PKR protein kinase by the nonstructural 5A protein, Virology 230 (1997) 217–227.
[8] D.R. Taylor, S.T. Shi, P.R. Romano, et al., Inhibition of the interferon-inducible protein kinase PKR by HCV E2 protein, Science 285 (1999) 107–110.
[9] M. Yoneyama, W. Suhara, Y. Fukuhara, et al., Direct triggering of the type I interferon system by virus infection: activation of a transcription factor complex containing IRF-3 and CBP/p300, Embo. J. 17 (1998) 1087–1095.
[10] J. Hiscott, Triggering the innate antiviral response through IRF-3 activation, J. Biol. Chem. 282 (2007) 15325–15329.
[11] E.F. Meurs, A. Breiman, The interferon inducing pathways and the hepatitis C virus, World J. Gastroenterol. 13 (2007) 2446–2454.
[12] E. Foy, K. Li, C. Wang, et al., Regulation of interferon regulatory factor-3 by the hepatitis C virus serine protease, Science 300 (2003) 1145–1148.
[13] E. Meylan, J. Curran, K. Hofmann, et al., Cardif is an adaptor protein in the RIG-I antiviral pathway and is targeted by hepatitis C virus, Nature 437 (2005) 1167–1172.
[14] X.D. Li, L. Sun, R.B. Seth, et al., Hepatitis C virus protease NS3/4A cleaves mitochondrial antiviral signaling protein off the mitochondria to evade innate immunity, Proc. Natl. Acad. Sci. USA 102 (2005) 17717–17722.
[15] R. Lin, J. Lacoste, P. Nakhaei, et al., Dissociation of a MAVS/IPS-1/VISA/Cardif-IKKepsilon molecular complex from the mitochondrial outer membrane by hepatitis C virus NS3-4A proteolytic cleavage, J. Virol. 80 (2006) 6072–6083.
[16] K. Li, E. Foy, J.C. Ferreon, et al., Immune evasion by hepatitis C virus NS3/4A protease-mediated cleavage of the Toll-like receptor 3 adaptor protein TRIF, Proc. Natl. Acad. Sci. USA 102 (2005) 2992–2997.
[17] R. Suzuki, Y. Matsuura, T. Suzuki, et al., Nuclear localization of the truncated hepatitis C virus core protein with its hydrophobic C terminus deleted, J. Gen. Virol. 76 (Pt 1) (1995) 53–61.
[18] W. Suhara, M. Yoneyama, I. Kitabayashi, et al., Direct involvement of CREB-binding protein/p300 in sequence-specific DNA binding of virus-activated interferon regulatory factor-3 holocomplex, J. Biol. Chem. 277 (2002) 22304–22313.
[19] M. Mori, M. Yoneyama, T. Ito, et al., Identification of Ser-386 of interferon regulatory factor 3 as critical target for inducible phosphorylation that determines activation, J. Biol. Chem. 279 (2004) 9698–9702.
[20] K. Tsukiyama-Kohara, S. Tone, I. Maruyama, et al., Activation of the CKI-CDK-Rb-E2F pathway in full genome hepatitis C virus-expressing cells, J. Biol. Chem. 279 (2004) 14531–14541.
[21] T. Nishimura, M. Kohara, K. Izumi, et al., Hepatitis C virus impairs p53 via persistent overexpression of 3beta-hydroxysterol Delta24-reductase, J. Biol. Chem. 284 (2009) 36442–36452.
[22] A.M. Owsianka, A.H. Patel, Hepatitis C virus core protein interacts with a human DEAD box protein DDX3, Virology 257 (1999) 330–340.
[23] M. Schroder, M. Baran, A.G. Bowie, Viral targeting of DEAD box protein 3 reveals its role in TBK1/IKKepsilon-mediated IRF activation, EMBO J. 27 (2008) 2147–2157.
[24] H. Oshiumi, K. Sakai, M. Matsumoto, T. Seya, DEAD/H BOX 3 (DDX3) helicase binds the RIG-I adaptor IPS-1 to up-regulate IFN-beta-inducing potential, Eur. J. Immunol. 40 (4) (2010) 940–948.
[25] P.C. Chang, C.W. Chi, G.Y. Chau, et al., DDX3, a DEAD box RNA helicase, is deregulated in hepatitis virus-associated hepatocellular carcinoma and is involved in cell growth control, Oncogene 25 (2006) 1991–2003.

Immunization with a Recombinant Vaccinia Virus That Encodes Nonstructural Proteins of the Hepatitis C Virus Suppresses Viral Protein Levels in Mouse Liver

Satoshi Sekiguchi[1], Kiminori Kimura[2], Tomoko Chiyo[1], Takahiro Ohtsuki[1], Yoshimi Tobita[1], Yuko Tokunaga[1], Fumihiko Yasui[1], Kyoko Tsukiyama-Kohara[3], Takaji Wakita[4], Toshiyuki Tanaka[5], Masayuki Miyasaka[6], Kyosuke Mizuno[7], Yukiko Hayashi[8], Tsunekazu Hishima[8], Kouji Matsushima[9], Michinori Kohara[1]*

1 Department of Microbiology and Cell Biology, Tokyo Metropolitan Institute of Medical Science, Setagaya-ku, Tokyo, Japan, **2** Division of Hepatology, Tokyo Metropolitan Komagome Hospital, Bunkyo-ku, Tokyo, Japan, **3** Transboundary Animal Diseases Center, Joint Faculty of Veterinary Medicine, Kagoshima University, Korimoto, Kagoshima, Japan, **4** Department of Virology II, National Institute of Infectious Diseases, Shinjuku-ku, Tokyo, Japan, **5** Laboratory of Immunobiology, Department of Pharmacy, School of Pharmacy, Hyogo University of Health Sciences, Chuo-ku, Kobe, Japan, **6** Laboratory of Immunodynamics, Department of Microbiology and Immunology, Osaka University Graduate School of Medicine, Suita, Osaka, Japan, **7** Chemo-Sero-Therapeutic Research Institute, Okubo, Kumamoto, Japan, **8** Department of Pathology, Tokyo Metropolitan Komagome Hospital, Bunkyo-ku, Tokyo, Japan, **9** Department of Molecular Preventive Medicine, School of Medicine, University of Tokyo, Bunkyo-ku, Tokyo, Japan

Abstract

Chronic hepatitis C, which is caused by infection with the hepatitis C virus (HCV), is a global health problem. Using a mouse model of hepatitis C, we examined the therapeutic effects of a recombinant vaccinia virus (rVV) that encodes an HCV protein. We generated immunocompetent mice that each expressed multiple HCV proteins via a Cre/*loxP* switching system and established several distinct attenuated rVV strains. The HCV core protein was expressed consistently in the liver after polyinosinic acid–polycytidylic acid injection, and these mice showed chronic hepatitis C-related pathological findings (hepatocyte abnormalities, accumulation of glycogen, steatosis), liver fibrosis, and hepatocellular carcinoma. Immunization with one rVV strain (rVV-N25), which encoded nonstructural HCV proteins, suppressed serum inflammatory cytokine levels and alleviated the symptoms of pathological chronic hepatitis C within 7 days after injection. Furthermore, HCV protein levels in liver tissue also decreased in a CD4 and CD8 T-cell-dependent manner. Consistent with these results, we showed that rVV-N25 immunization induced a robust CD8 T-cell immune response that was specific to the HCV nonstructural protein 2. We also demonstrated that the onset of chronic hepatitis in CN2-29$^{(+/-)}$/MxCre$^{(+/-)}$ mice was mainly attributable to inflammatory cytokines, (tumor necrosis factor) TNF-α and (interleukin) IL-6. Thus, our generated mice model should be useful for further investigation of the immunological processes associated with persistent expression of HCV proteins because these mice had not developed immune tolerance to the HCV antigen. In addition, we propose that rVV-N25 could be developed as an effective therapeutic vaccine.

Citation: Sekiguchi S, Kimura K, Chiyo T, Ohtsuki T, Tobita Y, et al. (2012) Immunization with a Recombinant Vaccinia Virus That Encodes Nonstructural Proteins of the Hepatitis C Virus Suppresses Viral Protein Levels in Mouse Liver. PLoS ONE 7(12): e51656. doi:10.1371/journal.pone.0051656

Editor: Naglaa H. Shoukry, University of Montreal, Canada

Received March 13, 2012; **Accepted** November 5, 2012; **Published** December 17, 2012

Funding: This study was supported by grants from the Ministry of Education, Culture, Sports, Science, and Technology of Japan; the Program for Promotion of Fundamental Studies in Health Sciences of the Pharmaceuticals and Medical Devices Agency of Japan; and the Ministry of Health, Labor, and Welfare of Japan. The funders had no role in study design, data collection and analysis, decision to publish, or preparation of the manuscript.

Competing Interests: The authors have declared that no competing interests exist.

* E-mail: kohara-mc@igakuken.or.jp

Introduction

Hepatitis C virus (HCV) is a major public health problem; approximately 170 million people are infected with HCV worldwide [1]. HCV causes persistent infections that can lead to chronic liver diseases such as chronic hepatitis, liver cirrhosis, and hepatocellular carcinoma (HCC) [2]. Antiviral drugs are not highly effective in individuals with a chronic infection; furthermore, an effective vaccine against HVC has not been developed. A convenient animal model of HCV infection will greatly facilitate the development of an effective HCV vaccine.

Transgenic mice that express HCV proteins have been generated to study HCV expression [3,4]; however, in each of these cases, the relevant transgenes is expressed during embryonic development; therefore, the transgenic mice become immunotolerant to the transgenic products, and consequently, the adult mice are not useful for investigations of the pathogenesis of chronic hepatitis C. To address this problem, we developed a system that can drive conditional expression of an HCV transgene; our system involves the Cre/*loxP* system and a recombinant adenovirus capable of expressing Cre recombinase [5,6]. Concerns have been expressed that an adenovirus and transient expression of HCV proteins could induce immune responses [5] and, therefore, obscure any evidence of the effect of the host immune responses on chronic liver pathology. Therefore, here, we used a Cre/*loxP* switching system to generate an immunocompetent mouse model

of HCV protein expression; with this system, we could study the host immune responses against HCV proteins.

Folgori et al. (2006) reported effective vaccination of chimpanzees with an adenoviral vector and plasmid DNA encoding the HCV nonstructural region. This technique protected the liver tissues from acute hepatitis, which results when whole animals are challenged with virus [7]. However, this vaccine has not yet been shown to be effective against chronic HCV infection.

Here, we aimed to address how HCV expression causes chronic liver diseases and to provide new options for HCV vaccine development. Using LC16m8, a highly attenuated strain of vaccinia virus (VV), we generated three recombinant vaccinia viruses (rVVs) that each encoded one of three different HCV proteins and found that one recombinant virus (rVV-N25), which encoded nonstructural HCV proteins, resolved pathological chronic hepatitis C symptoms in the liver. We also found that immunization with rVV-N25 suppressed HCV core protein levels in the livers of transgenic mice; moreover, this suppression was mediated by CD4 and CD8 T cells, as has been previously reported [8].

Results

Generation of a Model of Persistent HCV Protein Expression

To produce adult mice that express an HCV transgene, we bred CN2-29 transgenic mice, which carry an HCV transgene, [5,6,9] with Mx1-Cre transgenic mice [10], which express Cre recombinase in response to interferon (IFN)-α or a chemical inducer of IFN-α, poly(I:C) (Figure 1A). Following poly(I:C) injection, the HCV transgene was rearranged, and HCV sequences were expressed in the livers of F1 progeny (CN2-$29^{(+/-)}$/$MxCre^{(+/-)}$ mice) within 7 days after poly(I:C) injection (Figure 1B).

To evaluate the characteristic features of these CN2-$29^{(+/-)}$/$MxCre^{(+/-)}$ mice, we analyzed serum alanine aminotransferase (ALT) and liver HCV core protein levels after poly(I:C) injection. As illustrated in Figure 1C, serum ALT levels increased and reached a peak at 24 h after the first poly(I:C) injection; this elevation appeared to be a direct result of the poly(I:C) treatment, which causes liver injury [11]. After this peak, serum ALT levels dropped continuously until day 4, and then ALT levels began to increase, as did HCV core protein levels. Thereafter, the HCV core protein was expressed consistently for at least 600 days.

Histological analysis showed HCV core protein expression in most hepatocytes of the transgenic mice; these mice showed evidence of lymphocytic infiltration that was caused by the HCV core proteins (Figure 1D and E). These observations, in addition to the modified histology activity index (HAI) scores, indicated that expression of HCV proteins caused chronic hepatitis in the CN2-$29^{(+/-)}$/$MxCre^{(+/-)}$ mice because a weak, though persistent, immune response followed an initial bout of acute hepatitis (Figure S1). Moreover, we observed a number of other pathological changes in these mice – including swelling of hepatocytes, abnormal architecture of liver-cell cords, abnormal accumulation of glycogen, steatosis, fibrosis, and HCC (Figures 1E and F, Table S1). Steatosis was mild in the younger mice (day 21) and became increasingly severe over time (days 120 and 180; Figure S2). Importantly, none of the pathological changes were observed in the CN2-$29^{(+/-)}$/$MxCre^{(-/-)}$ mice after poly(I:C) injection (Figure 1F).

Recombinant Vaccinia Virus Immunization in HCV Transgenic Mice

To determine whether activation of the host immune response caused the reduction with HCV protein levels in the livers of CN2-$29^{(+/-)}$/$MxCre^{(+/-)}$ mice, we used a highly attenuated VV strain, LC16m8, to generate three rVVs [12]. Each rVV encoded a different HCV protein; rVV-CN2 encoded mainly structural proteins, rVV-N25 encoded nonstructural proteins, and rVV-CN5 encoded the entire HCV protein region (Figure 2A). Because rVVs can express a variety of proteins and induce strong and long-term immunity, they have been evaluated as potential prophylactic vaccines [13].

We used western blots to confirm that each HCV protein was expressed in cell lines. Each of seven proteins – the core, E1, E2, NS3-4A, NS4B, NS5A, and NS5B – was recognized and labeled by a separate cognate antibody directed (Figure S3). To induce effective immune responses against HCV proteins in transgenic mice, we injected an rVV-HCV (rVV-CN2, rVV-CN5, or rVV-N25) or LC16m8 (as the control) intradermally into CN2-$29^{(+/-)}$/$MxCre^{(+/-)}$ mice 90 days after poly(I:C) injection (Figure 2B). Analysis of liver sections 7 days after immunization with rVV-N25 revealed dramatic improvement in a variety of pathological findings associated with chronic hepatitis – including piecemeal necrosis, hepatocyte swelling, abnormal architecture of liver-cell cords, abnormal accumulation of glycogen, and steatosis (Figures 2C–E). Collectively, these results demonstrated that only the rVV-N25 treatment resulted in histological changes indicative of improvement in the chronic hepatitis suffered by the transgenic mice.

To determine whether rVV-N25 treatment induced the same effect in other strains of HCV transgenic mice, we analyzed RzCN5-$15^{(+/-)}$/$MxCre^{(+/-)}$ mice, which express all HCV proteins; in these mice, chronic hepatitis was resolved within 28 days of immunization with rVV-N25. Taken together, these findings indicated that rVV-N25 had a dramatic therapeutic effect on both types of HCV transgenic mice (Figure S4).

Treatment with rVV-N25 Reduced the HCV Core Protein Levels in the Livers

To assess in detail the effects of rVV-HCV immunization on HCV protein clearance from the livers of CN2-$29^{(+/-)}$/$MxCre^{(+/-)}$ mice, we monitored the levels of HCV core protein in liver samples via ELISA. We found that within 28 days after immunization the HCV core protein levels were significantly lower in livers of rVV-N25-treated mice than in those of control mice (Figure 3A). Immunohistochemical analysis indicated that, within 28 days after immunization, levels of HCV core protein were substantially lower in the livers of CN2-$29^{(+/-)}$/$MxCre^{(+/-)}$ mice than in those of control mice (Figure 3B). Importantly, neither resolution of chronic hepatitis nor reduction in the HCV protein levels was observed in the mice treated with LC16m8, rVV-CN2, or rVV-CN5. These results indicated that HCV nonstructural proteins might be important for effects of therapeutic vaccines. In contrast, rVV-CN5 which encoded HCV structural and non-structural proteins did not show any significant effects. These results indicated that HCV structural proteins might have inhibited the therapeutic effects of the non-structural proteins. Therefore, it may be important to exclude the HCV structural proteins (aa 1–541) as antigenic proteins when developing therapeutic vaccines against chronic hepatitis C.

In addition, we measured serum ALT levels in CN2-$29^{(+/-)}$/$MxCre^{(+/-)}$ mice from all four treatment groups 28 days after rVV-HCV immunization. Serum ALT levels were not significant-

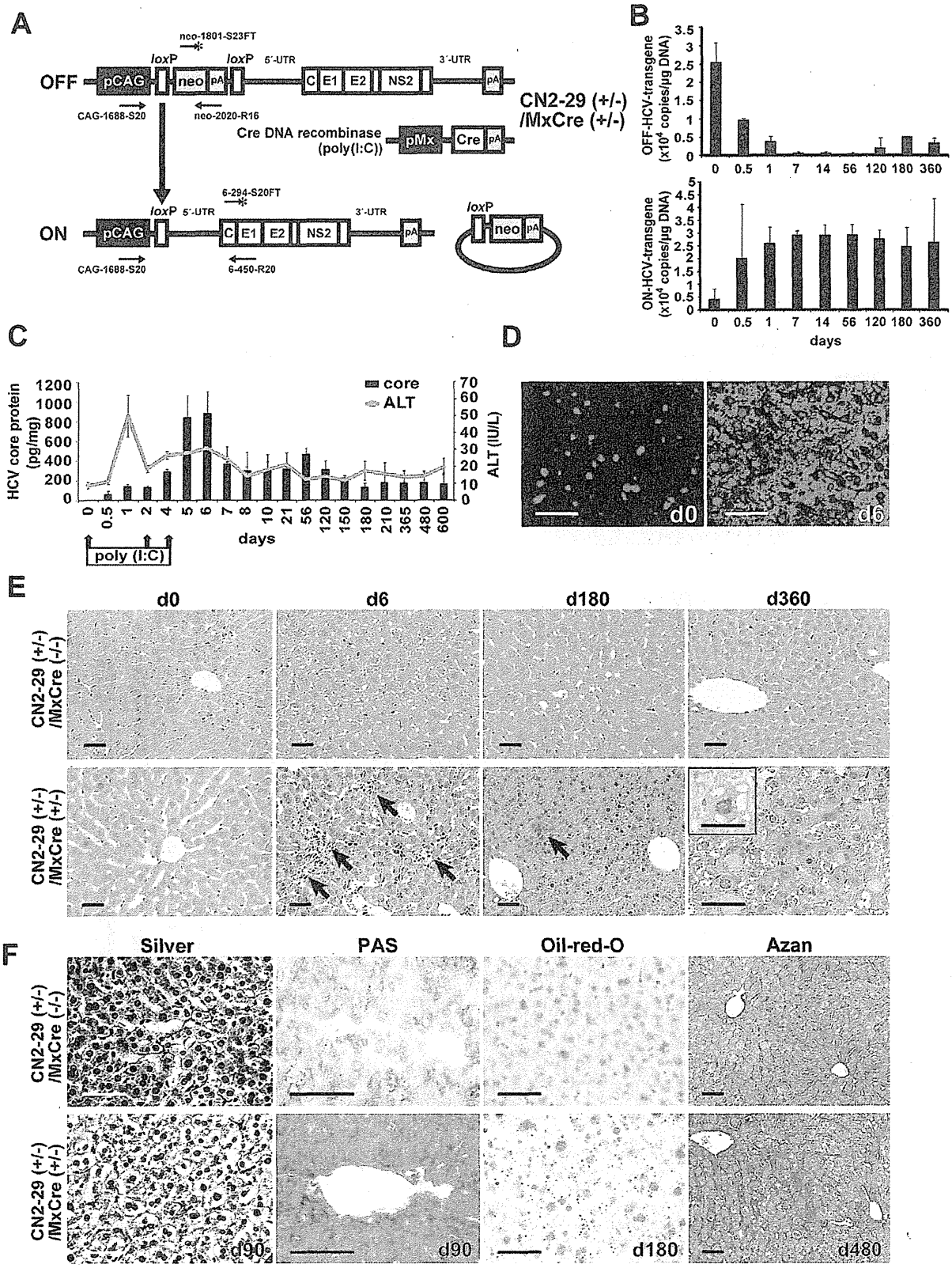
A
neo-1801-S23FT
loxP
loxP
5'-UTR
3'-UTR
OFF
pCAG
neo
pA
C
E1
E2
NS2
pA
CAG-1688-S20
neo-2020-R16
CN2-29 (+/-)
/MxCre (+/-)
Cre DNA recombinase
(poly(I:C))
pMx
Cre
pA
6-294-S20FT
ON
6-450-R20
B
OFF-HCV-transgene
(x10⁴ copies/μg DNA)
ON-HCV-transgene
(x10⁴ copies/μg DNA)
0 0.5 1 7 14 56 120 180 360
days
C
HCV core protein
(pg/mg)
core
ALT
ALT (IU/L)
0 0.5 1 2 4 5 6 7 8 10 21 56 120 150 180 210 365 480 600
days
poly (I:C)
D
d0
d6
E
d0
d6
d180
d360
CN2-29 (+/-)
/MxCre (-/-)
CN2-29 (+/-)
/MxCre (+/-)
F
Silver
PAS
Oil-red-O
Azan
d90
d90
d180
d480

Figure 1. Pathogenesis in immunocompetent mice with persistent HCV expression. (**A**) Structure of CN2-29$^{(+/-)}$/MxCre$^{(+/-)}$ and the Cre-mediated activation of the transgene unit. R6CN2 HCV cDNA was cloned downstream of the CAG promoter, neomycin-resistant gene (*neo*), and poly A (pA) signal flanked by two *loxP* sequences. This cDNA contains the core, E1, E2, and NS2 regions. (**B**) Cre-mediated genomic DNA recombination. After poly(I:C) injection, genomic DNA was extracted from liver tissues and analyzed by quantitative RTD-PCR for Cre-mediated transgenic recombination. The transgene was almost fully recombined in transgenic mouse livers 7 days after the injection. In all cases, n = 3 mice per group. (**C**) HCV core protein expression was sustained for at least 600 days after poly(I:C) injection. (**D**) Immunohistochemical analysis revealed that most hepatocytes expressed the HCV core protein within 6 days after injection. (**E**) Liver sections from CN2-29$^{(+/-)}$/MxCre$^{(+/-)}$ mice after the poly(I:C) injection. Infiltrating lymphocytes (arrows) were observed on days 6 and 180; Hepatocellular carcinoma (HCC) was observed on day 360. In contrast, these pathological changes were not observed in CN2-29$^{(+/-)}$/MxCre$^{(-/-)}$ mice after the injection. The inset image shows abnormal mitosis in a tumor cell. (**F**) Hepatocyte swelling and abnormal architecture of liver-cell cords (silver staining), as well as abnormal glycogen accumulation (PAS staining) were observed on day 90 in CN2-29$^{(+/-)}$/MxCre$^{(+/-)}$ mice. We observed steatosis (oil-red-O staining) on day 180 and, subsequently, fibrosis (Azan staining) on day 480. The scale bars indicate 50 μm.
doi:10.1371/journal.pone.0051656.g001

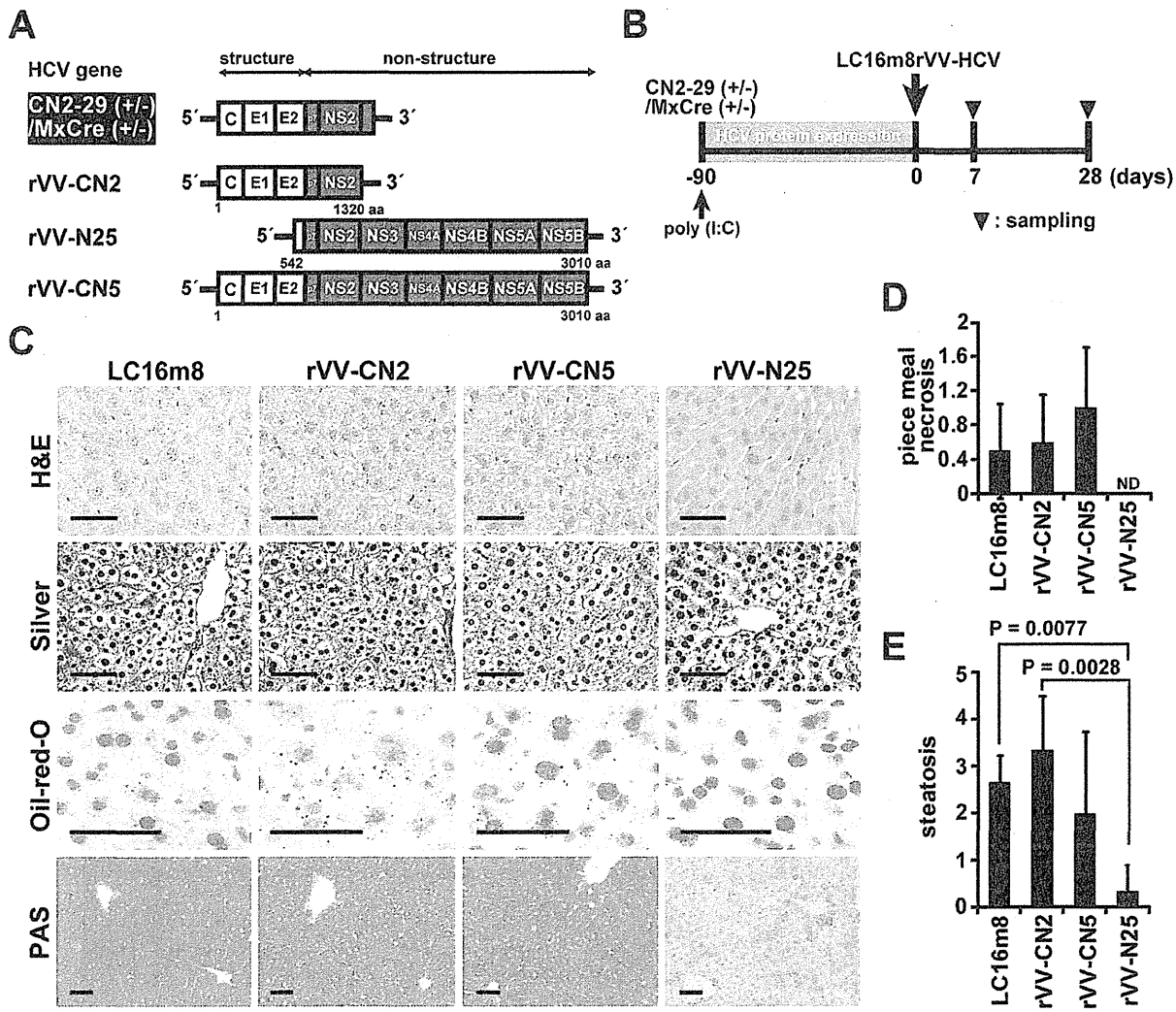

Figure 2. Effects of rVV-HCV treatment on the CN2-29$^{(+/-)}$/MxCre$^{(+/-)}$ mice. (**A**) HCV gene structure in the CN2-29$^{(+/-)}$/MxCre$^{(+/-)}$ mice and recombinant vaccinia viruses (rVV-HCV). MxCre/CN2-29 cDNA contains the core, E1, E2, and NS2 regions. The rVV-CN2 cDNA contains the core, E1, E2, and NS2 regions. The rVV-N25 cDNA contains the NS2, NS3, NS4A, NS4B, NS5A, and NS5B regions. The rVV-CN5 cDNA contains the entire HCV region. (**B**) Four groups of CN2-29$^{(+/-)}$/MxCre$^{(+/-)}$ mice were inoculated intradermally with rVV-CN2, rVV-N25, rVV-CN5, or LC16m8 90 days after the poly(I:C) injection. Blood, liver, and spleen tissue samples were collected 7 and 28 days after the inoculation. (**C**) Liver sections from the four groups of CN2-29$^{(+/-)}$/MxCre$^{(+/-)}$ mice 7 days after the inoculation. The sections were stained with H&E, silver, oil-red-O, or PAS. The scale bars indicate 50 μm. (**D**) Histological evaluation of piecemeal necrosis in the four groups of CN2-29$^{(+/-)}$/MxCre$^{(+/-)}$ mice 7 days after inoculation. (**E**) Histological evaluation of steatosis in the four groups of CN2-29$^{(+/-)}$/MxCre$^{(+/-)}$ mice 7 days after inoculation. Significant relationships are indicated by a P-value.
doi:10.1371/journal.pone.0051656.g002

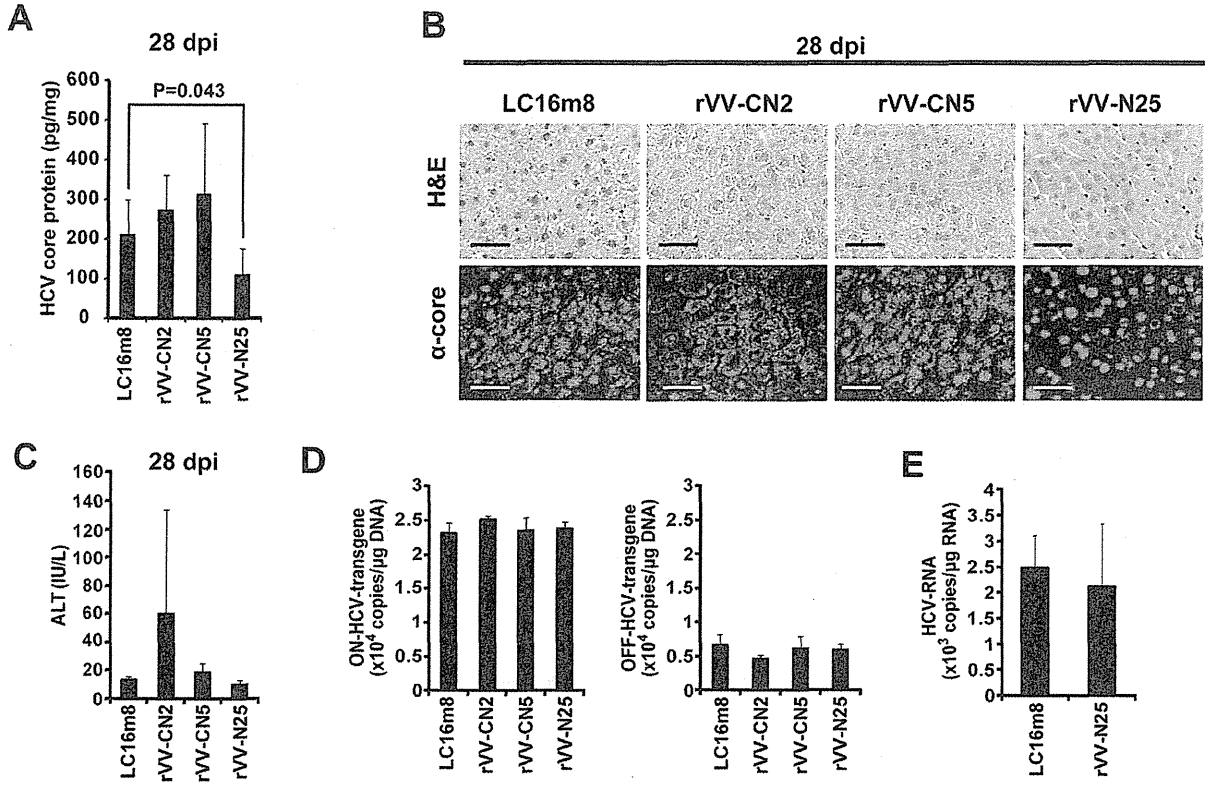

Figure 3. Effects of HCV core protein expression on the livers of CN2-29$^{(+/-)}$/MxCre$^{(+/-)}$ mice inoculated with rVV-HCV. (**A**) Expression of the HCV core protein in the four treatment groups of CN2-29$^{(+/-)}$/MxCre$^{(+/-)}$ mice 28 days after the inoculation. Significant relationships are indicated by a P-value. (**B**) H&E staining and immunohistochemical analysis for HCV core protein in the LC16m8-, rVV-CN2-, rVV-CN5-, or rVV-N25-treated CN2-29$^{(+/-)}$/MxCre$^{(+/-)}$ mice 28 days after the inoculation. Liver sections were stained with the anti-core monoclonal antibody. The scale bars indicate 50 μm. (**C**) Effects of HCV core protein expression on serum ALT levels in the four treatment groups of CN2-29$^{(+/-)}$/MxCre$^{(+/-)}$ mice 28 days after immunization. (**D**) Cre-mediated genomic DNA recombination in the four treatment groups 28 days after immunization. (**E**) Expression of HCV mRNA in the LC16m8- or rVV-N25-treated CN2-29$^{(+/-)}$/MxCre$^{(+/-)}$ mice 28 days after immunization. In all cases, n = 6 mice per group.
doi:10.1371/journal.pone.0051656.g003

ly different in the rVV-N25-treated mice and control mice (Figure 3C); this finding indicated that rVV-N25 treatment did not cause liver injury and that the antiviral effect was independent of hepatocyte destruction.

We hypothesized that the reduction in the levels of HCV core protein in rVV-HCV-treated mice was not caused by cytolytic elimination of hepatocytes that expressed HCV proteins. To investigate this hypothesis, we conducted an RTD-PCR analysis of genomic DNA from liver samples of CN2-29$^{(+/-)}$/MxCre$^{(+/-)}$ mice. The recombined transgene was similar in rVV-N25-treated and control mice 28 days after immunization (Figure 3D). We also measured the expression of HCV mRNA in LC16m8-treated CN2-29$^{(+/-)}$/MxCre$^{(+/-)}$ mice with that in rVV-N25-treated CN2-29$^{(+/-)}$/MxCre$^{(+/-)}$ mice 28 days after immunization; the HCV mRNA levels did not differ between rVV-N25-treated CN2-29$^{(+/-)}$/MxCre$^{(+/-)}$ and control mice (Figure 3E). These results indicated that rVV-N25-induced suppression of HCV core protein expression could be controlled at a posttranscriptional level.

Role of CD4 and CD8 T cells in rVV-N25-treated Mice

Viral clearance is usually associated with CD4 and CD8 T-cell activity that is regulated by cytolytic or noncytolytic antiviral mechanism [14]. To determine whether CD4 or CD8 T-cell activity was required for the reduction in HCV core protein levels in the livers of transgenic mice, we analyzed the core protein levels in CN2-29$^{(+/-)}$/MxCre$^{(+/-)}$ mice immunized with rVV-N25 in the absence of CD4 or CD8 T cells (Figure 4A). As expected, the mice lacking CD4 or CD8 T cells failed to show a reduction in HCV core protein levels (Figure 4B).

However, in mice lacking either CD4 or CD8 T-cells, the pathological changes associated with chronic hepatitis were resolved following rVV-N25 immunization, and the steatosis score of rVV-N25-treated mice was significantly lower than that of control mice (Figures 4C–E). These results indicated that CD4 and CD8 T cells were not responsible for the rVV-N25-induced amelioration of histological findings and that other inflammatory cell types may play an as-yet-unidentified role in the resolution of the pathological changes in these mice.

rVV-N25 Immunization Induced an NS2-specific Activated CD8 T cells Response

Because we found that HCV protein reduction in the liver required CD8 T cells, we tested whether HCV-specific CD8 T cells were present in splenocytes 28 days after immunization. To determine the functional reactivity of HCV-specific CD8$^+$ T cells, we performed a CD107a mobilization assay and intracellular IFN-γ staining. CN2-29 transgenic mice expressed the HCV structural protein and the NS2 region. However, rVV-N25 comprised only

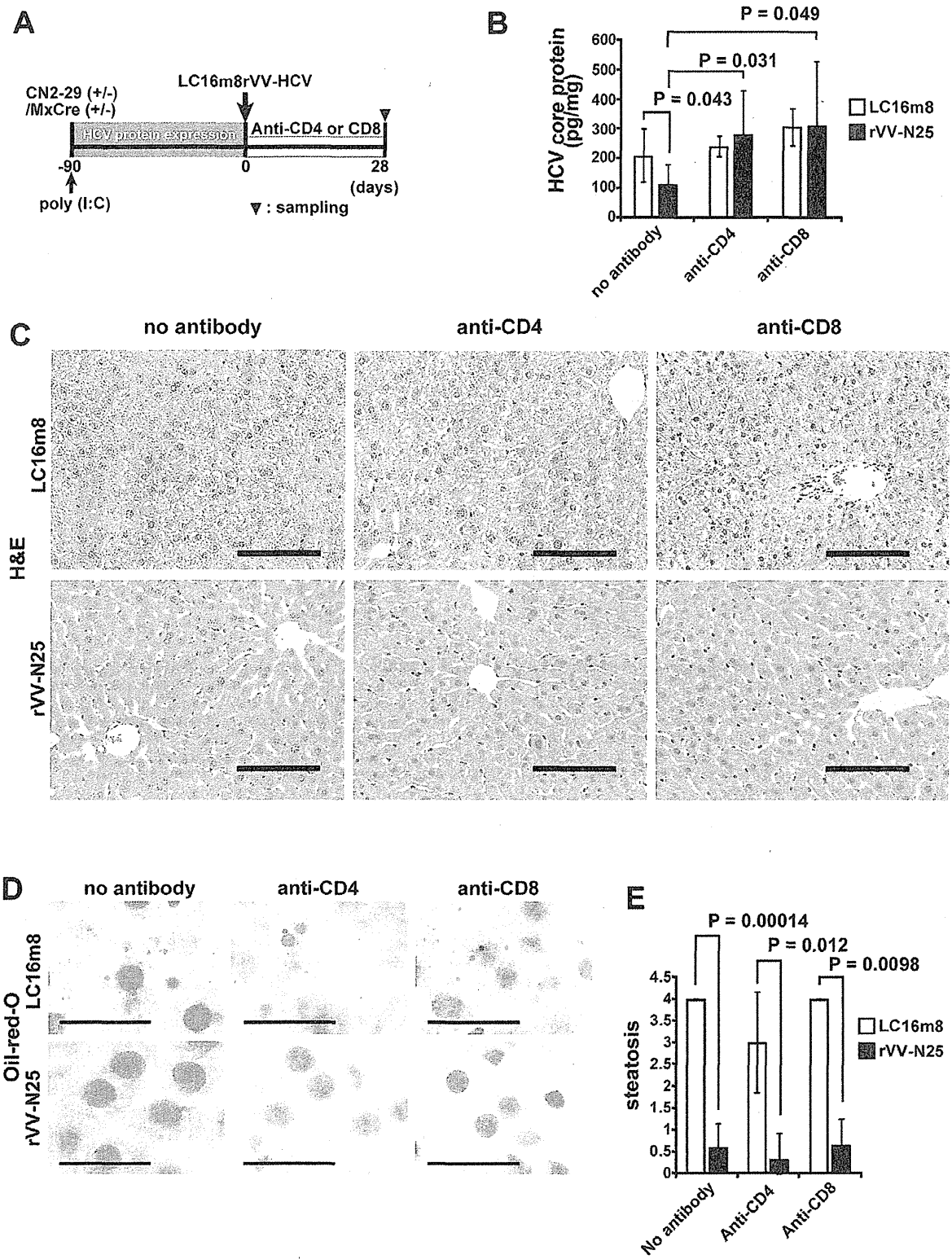

Figure 4. Role of CD4 and CD8 T cells in rVV-N25-treated mice. (**A**) Schematic diagram depicts depletion of CD4 and CD8 T cells via treatment with monoclonal antibodies. (**B**) Comparison of HCV core protein expression in control, CD4-depleted, and CD8-depleted mice 28 days after immunization with LC16m8 or rVV-N25. (**C, D**) Histological analysis of liver samples from CD4-depleted or CD8-depleted CN2-29$^{(+/-)}$/MxCre$^{(+/-)}$ mice

28 days after immunization with LC16m8 or rVV-N25. The scale bars indicate 100 μm (**C**) and 50 μm (**D**). (**E**) Histological evaluation of steatosis in liver samples from CD4-depleted or CD8-depleted CN2-29$^{(+/-)}$/MxCre$^{(+/-)}$ mice 28 days after immunization with LC16m8 or rVV-N25. Significant relationships are indicated by a P-value.
doi:10.1371/journal.pone.0051656.g004

a HCV nonstructural protein. Thus, we focused on the role of the NS2 region as the target for CD8 T cells and generated EL-4 cell lines that expressed the NS2 antigen or the CN2 antigen.

Isolated splenocytes from immunized mice were co-cultured with EL-4CN2 or EL-4NS2 cell lines for 2 weeks and analyzed.

Cytolytic cell activation can be measured using CD107a, a marker of degranulation [15]. The ratio of CD8$^+$CD107a$^+$ cells to all CD8 T cells significantly increased in rVV-N25-treated splenocytes after co-culture with EL-4CN2 or EL-4NS2 ($P<0.05$), whereas splenocytes that had been treated with any other rVV were not detected (Figure 5A, B and C). These results indicated that rVV-N25 treatment increased the frequency of HCV NS2-specific activated CD8 T cells. Consistent with these results, the ratio of CD8$^+$IFN-γ$^+$ cells to all CD8 T cells for rVV-N25-treated mice was also significantly higher than that for mice treated with any other rVV ($P<0.05$). Taken together, these findings indicated that rVV-N25 induced an effective CD8 T-cell immune response and that NS2 is an important epitope for CD8 T cells.

rVV-N25 Immunization Suppressed Inflammatory Cytokines Production

To determine whether rVV-N25 treatment affected inflammatory cytokine production, we measured serum levels of inflammatory cytokines after rVV immunization. The serum levels of these inflammatory cytokines increased in the CN2-29$^{(+/-)}$/MxCre$^{(+/-)}$ mice (Figure 6A, Figure S5). Immunization with rVV-N25 affected serum levels of inflammatory cytokines in CN2-29$^{(+/-)}$/MxCre$^{(+/-)}$ mice and caused a return to the cytokine levels observed in wild-type untreated mice (Figure 6A). In wild-type mice, the cytokine levels remained unchanged after immunization (Figure 6A). These results indicated that inflammatory cytokines were responsible for liver pathogenesis in the transgenic mice.

To test the hypothesis that inflammatory cytokines were responsible for liver pathogenesis in CN2-29$^{(+/-)}$/MxCre$^{(+/-)}$ mice, we administered transgenic mouse serum intravenously into nontransgenic mice. We observed the development of chronic hepatitis in the nontransgenic mice within 7 days after the serum transfer (Figures 6B and C). This finding was consistent with the

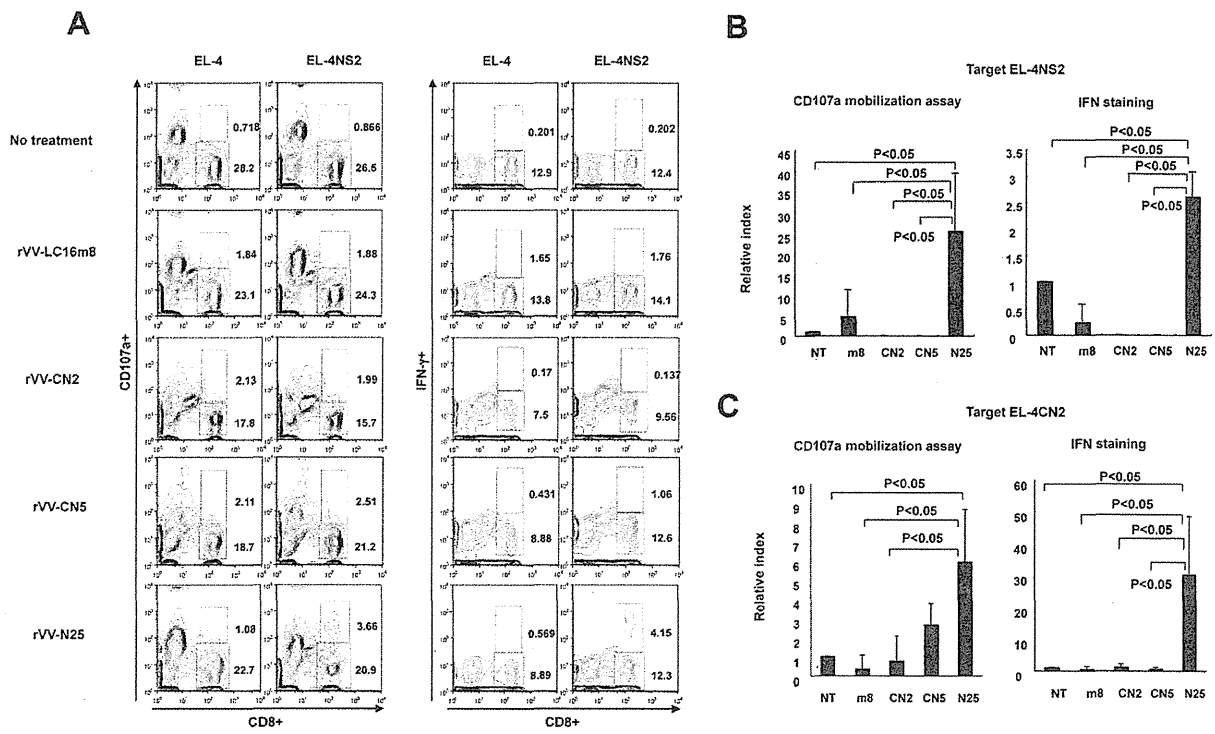

Figure 5. Immunization with rVV-N25 induced CD8 T-cell degranulation, a marker for cytotoxicity, and IFN-γ production. (**A**) The numbers represent the percentage of CD107a positive cells and negative cells (left two columns) and IFN-γ-positive cells and negative cells (right two columns). (**B, C**) The ratio of CD8$^+$IFN-γ$^+$ cells to all CD8 T cells for rVV-N25-treated mice was significantly higher than that for mice treated with any other rVV. Splenocytes (4 × 10^6 per well) were cultured with EL-4CN2 or EL-4NS2 cell lines in RPMI 1640 complete medium including 3% T-STIM^{TM} with ConA for 2 weeks. Harvested cells were incubated for 4 h with EL-4, EL-4CN2, or EL-4NS2 in combination with PE-labeled anti-CD107a mAb and monensin in RPMI 1640 complete medium with 50 IU/mL IL-2, according to the manufacturer's instruction. After incubation, cell suspensions were washed with PBS, and the cells were further stained with APC-labeled anti-IFN-γ mAb and Pacific blue-labeled anti-CD8 mAb. Harvested cells were stained with anti-CD107a-PE, anti-IFN-γ-APC, or anti-CD8-Pacific blue. Results that are representative of three independent experiments are shown. Significant relationships are indicated by P-value.
doi:10.1371/journal.pone.0051656.g005

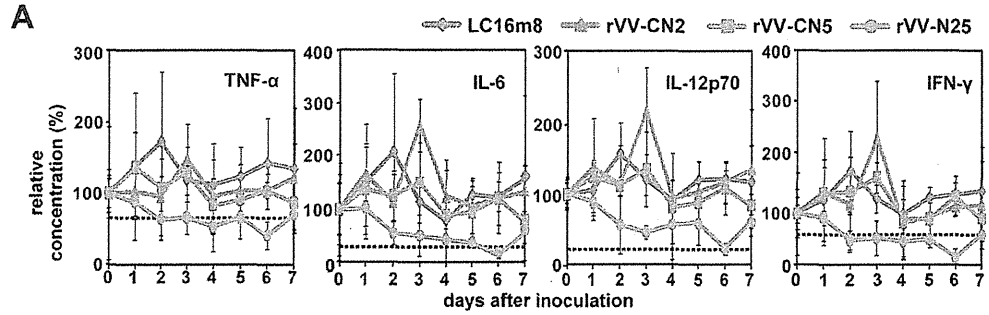
A
LC16m8
rVV-CN2
rVV-CN5
rVV-N25
TNF-α
IL-6
IL-12p70
IFN-γ
relative concentration (%)
days after inoculation

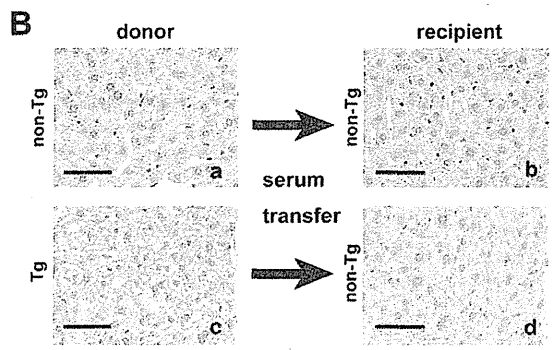
B
donor
recipient
non-Tg
Tg
serum transfer
a
b
c
d

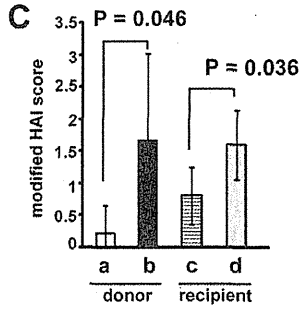
C
P = 0.046
P = 0.036
modified HAI score
a b c d
donor
recipient

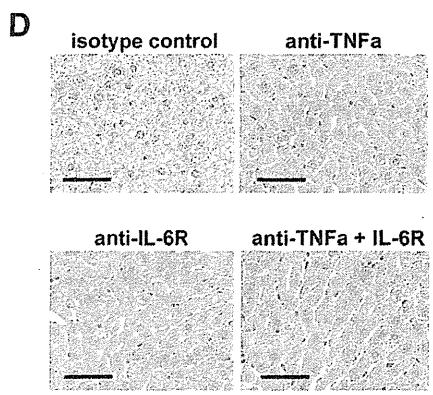
D
isotype control
anti-TNFa
anti-IL-6R
anti-TNFa + IL-6R

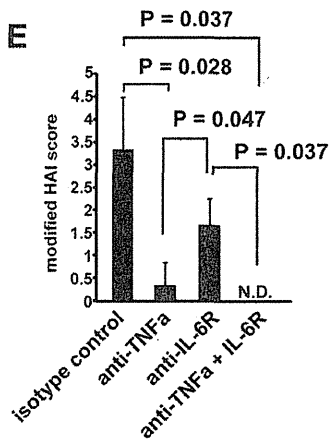
E
P = 0.037
P = 0.028
P = 0.047
P = 0.037
modified HAI score
N.D.
isotype control
anti-TNFa
anti-IL-6R
anti-TNFa + IL-6R

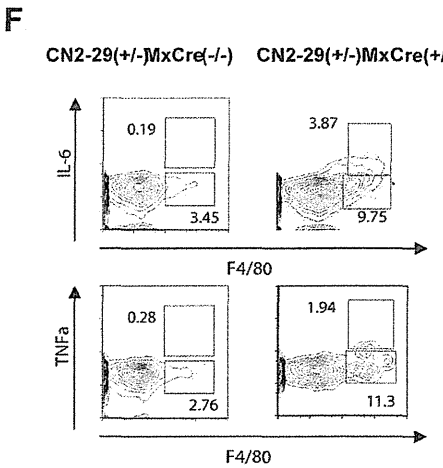
F
CN2-29(+/-)MxCre(-/-)
CN2-29(+/-)MxCre(+/-)
IL-6
TNFa
F4/80
0.19
3.45
3.87
9.75
0.28
2.76
1.94
11.3

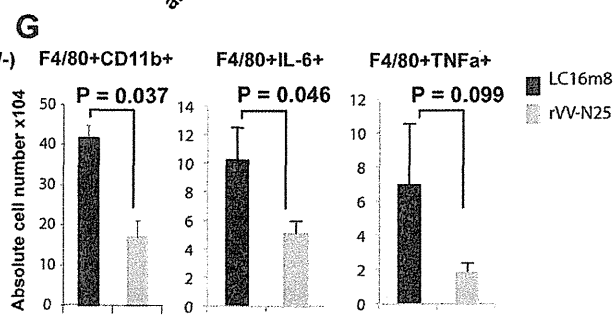
G
F4/80+CD11b+
F4/80+IL-6+
F4/80+TNFa+
P = 0.037
P = 0.046
P = 0.099
Absolute cell number x104
LC16m8
rVV-N25

Figure 6. Immunization with rVV-N25 suppresses serum inflammatory cytokine levels. (**A**) Daily cytokine levels in the serum of CN2-29$^{(+/-)}$/MxCre$^{(+/-)}$ mice during the week following immunization with LC16m8, rVV-CN2, rVV-N25, or rVV-CN5. Values represent means ± SD (n = 3) and reflect the concentrations relative to those measured on day 0. The broken lines indicate the baseline data from wild-type mice. In all cases, n = 6 mice per group. (**B**) Liver sections from CN2-29$^{(+/-)}$/MxCre$^{(+/-)}$ and CN2-29$^{(+/-)}$/MxCre$^{(-/-)}$ mice. (**C**) Histology activity index (HAI) scores of liver samples taken from CN2-29$^{(+/-)}$/MxCre$^{(+/-)}$, or CN2-29$^{(+/-)}$/MxCre$^{(-/-)}$ mice. (**D**) Liver sections from CN2-29$^{(+/-)}$/MxCre$^{(+/-)}$ mice in which TNF-α was neutralized and the IL-6 receptor was blocked. The scale bars indicate 50 μm. (**E**) HAI scores of liver samples taken from CN2-29$^{(+/-)}$/MxCre$^{(+/-)}$ in which TNF-α was neutralized and the IL-6 receptor was blocked. Tg and non-Tg indicate CN2-29$^{(+/-)}$/MxCre$^{(+/-)}$ and CN2-29$^{(+/-)}$/MxCre$^{(-/-)}$, respectively. (F) Macrophages were the main producers of TNF-α and IL-6 in CN2-29$^{(+/-)}$/MxCre$^{(+/-)}$ mice following poly(I:C) injection. (G) Immunization with rVV-N25 reduced the number of macrophages in liver samples from CN2-29$^{(+/-)}$/MxCre$^{(+/-)}$ mice and suppressed TNF-α and IL-6 production from macrophages (Figure 6G). Significant relationships are indicated by a P-value.
doi:10.1371/journal.pone.0051656.g006

hypothesis that inflammatory mediators played a key role in inducing hepatitis. Furthermore, to investigate whether TNF-α and IL-6 played particularly critical roles in the pathogenesis of chronic hepatitis in the transgenic mice, we neutralized TNF-α and blocked the IL-6 receptor in the livers of these mice. As expected, chronic hepatitis did not develop in these mice. (Figure 6D and E).

Next, to determine which cell population(s) produced TNF-α, IL-6, or both during continuous HCV expression in CN2-29$^{(+/-)}$/MxCre$^{(+/-)}$ mice, we isolated intrahepatic lymphocytes (IHLs) and labeled the macrophages (the F4/80^{+} cells) with anti-TNF-α and anti-IL-6 antibodies using an intracellular cytokine detection method. Macrophages in CN2-29$^{(+/-)}$/MxCre$^{(-/-)}$ mice produced small amounts of TNF-α and IL-6, while those in CN2-29$^{(+/-)}$/MxCre$^{(+/-)}$ mice produced much larger amounts of these cytokines (Figure 6F).

Finally, we evaluated whether rVV-N25 treatment affected the number of macrophages, cytokine production by macrophages, or both; specifically, we isolated IHLs from CN2-29$^{(+/-)}$/MxCre$^{(+/-)}$ mice 7 days after immunization with rVV-N25 or with LC16m8. The percentage of macrophages (CD11b^{+}F4/80^{+}) among IHLs and IL-6 production from these macrophages were significantly lower in rVV-N25-treated mice than in control mice (Figure 6G). Though the percentage of TNF-α-producing macrophages was not significantly different in rVV-N25-treated and control mice (P = 0.099), rVV-N25 treatment appeared to suppress these macrophages. These results demonstrated that rVV-N25 had a suppressive effect on activated macrophages, and they indicated that this suppression ameliorated the histological indicators of chronic hepatitis.

Discussion

Various HCV transgenic mouse models have been developed and used to examine immune response to HCV expression and the effects of pathogenic HCV protein on hepatocytes [4,16,17]. However, these transgenic mice develop tolerance to the HCV protein; therefore, examining immune response to HCV protein has been difficult.

To overcome the problem of immune tolerance in mouse models of HCV expression, we developed an HCV model in mice that relies on conditional expression of the core, E1, E2, and NS2 proteins and the Cre/loxP switching system [5,6]; we showed that the injection of an Ad-Cre vector enhanced the frequency of HCV-specific activated CD8 T cells in the liver of these mice and caused liver injury. However, the Ad-Cre adenovirus vector alone causes acute hepatitis in wild-type mice. Nevertheless, the transgenic model was useful for evaluating interactions between the host immune system and viral protein (serum ALT level over 2,000 IU/L) [5]; HCV core protein levels were reduced and expression of this protein was transient (about 2 weeks). Therefore, this Ad-Cre-dependent model cannot be used to effectively investigate immune responses to chronic HCV hepatitis.

Here, we used poly (I:C)-induced expression of Cre recombinase to generate HCV transgenic mice in order to study the effect of HCV protein and confirmed that these mice developed chronic active hepatitis–including steatosis, lipid deposition, and hepatocellular carcinoma. These pathological findings in the transgenic mice were very similar to those in humans with chronic hepatitis C; therefore, this mouse model of HCV may be useful for analyzing the immune response to chronic hepatitis. However, experimental results obtained with this mouse model may not directly translate to clinical findings from patients with HCV infection because the expression of HCV proteins was not liver specific in these mice. Furthermore, poly(I:C) injection can activate innate immune responses and, consequently, might induce temporary liver injury [18]. Additionally, poly(I:C) injection has an adjuvant effect; specifically, it stimulates TLR3 signaling [19].

To evaluate whether poly(I:C) injection caused hepatitis in CN2-29$^{(+/-)}$/MxCre$^{(-/-)}$ mice, we examined serum ALT levels and liver histology following poly(I:C) injection. We found that, following poly(I:C) injection, serum ALT levels in CN2-29$^{(+/-)}$/MxCre$^{(-/-)}$ mice increased, reached a peak one day after injection, declined from day 1 to day 6, and were not elevated thereafter; this time-course indicated that poly(I:C) injection alone did not induced continuous liver injury (figure S6). Based on these findings, we believe that the effects of poly(I:C) injection in these mice did not confound our analysis of chronic hepatitis.

Immunization with rVV-N25 suppressed HCV protein levels in the liver, and this suppression was associated with ameliorated pathological chronic hepatitis findings (see Figure 3). Importantly, rVV-N25 treatment did not cause liver injury based on the serum ALT levels; therefore, this treatment was unlikely to have cytopathic effects on infected hepatocytes. These findings provided strong evidence that rVV-N25 treatment effectively halted the progression of chronic hepatitis. Immunization with plasmid DNA or with recombinant vaccinia virus can effectively induce cellular and humoral immune responses and exert a protective effect against challenge with HCV infection [20,21]. However, findings from these previous studies revealed HCV immunization of both uninfected, naïve animals and immune-tolerant animals induced a HCV-specific immune response. In the model describe here; the animals were immune competent for HCV; therefore, our findings provided further important evidence that rVV-N25 was effective in the treatment of chronic hepatitis.

In addition, we demonstrated that rVV-N25 treatment in the absence of CD4 and CD8 T cells had no effect on HCV clearance. This important observation indicated that rVV-N25-induced HCV clearance was mediated by CD4 and CD8 T cells. Many studies have shown that spontaneous viral clearance during acute HCV infection is characterized by a vigorous, broadly reactive CD4 and CD8 T-cell response. [8,22] HCV clearance and hepatocellular cytotoxicity are both mediated by CD8 antigen-specific (cytotoxic T lymphocyte) CTLs [23]. Consistent with these observations, rVV-N25 treatment effectively induced the accumulation of NS2-specific CD8 T cells, which express high levels of

CD107a and IFN-γin the spleen. Notably, even with rVV-N25 immunization, the frequency of activated CD8 T cells was very low, and a minimum of 2-weeks incubation was required to distinguish the difference between rVV treatments. Even if a small population of specific CD8+ T cells played a relevant role in the reduction of core protein, it is difficult to assert that the only NS2-specific CD8+ T cells were important to this reduction. However, based on the results presented in Figure 4B, we are able to conclude that at least CD8+ and/or CD4+ T cells were important to the reduction in HCV core protein. Therefore, to elucidate the mechanism of HCV protein clearance, further investigation of not only the other T cell epitopes but also other immunocompetent cells is required.

Interestingly, rVV-N25 treatment–but not the rVV-CN2 or rVV-CN5 treatment–efficiently induced a HCV-specific activated CD8 T cells response; this difference in efficacy could have one or more possible causes. The HCV structural proteins (core, E1, and E2 proteins) in the rVV-CN construct may cause the difference; Saito et al. reported that injection with plasmid constructs encoding the core protein induced a specific CTL response in BALB/c mice [24]. Reportedly, CTL activity against core or envelope protein is completely absent from transgenic mice immunized with a plasmid encoding the HCV structural proteins, but core-specific CTL activity is present in transgenic mice that were immunized with a plasmid encoding the HCV core [21]. In contrast, when recombinant vaccinia virus expressing different regions of the HCV polyprotein were injected into BALB/c mice, only the HCV core protein markedly suppressed vaccinia-specific CTL responses [25]. Thus, the HCV core protein may have an immunomodulatory function [26]. Based on these reports and our results, we hypothesize that the causes underlying the effectiveness of rVV-N25 treatment were as follows: 1) this rVV construct included the core and envelope proteins and 2) the core protein had an immune-suppressive effect on CTL induction. Therefore, we suggest that exclusion of the core and envelope antigen as immunogen is one important factor in HCV vaccine design.

Interestingly, immunization with rVV-N25 rapidly suppressed the inflammatory response; however, immunization with either of the other rVVs did not (see Figure 6A). This result indicated that rVV-N25 may modulate inflammation via innate immunity, as well as via acquired immunity. Reportedly, Toll-like receptor (TLR)-dependent recognition pathways play a role in the recognition of poxviruses [27]. TLR2 and TLR9 have also been implicated in the recognition of the vaccinia virus [28,29]. These findings indicate that TLR on dendritic cells may modulate the immunosuppressive effect of rVV-N25 in our model of HCV infection; however, further examination of this hypothesis is required. The finding that pathological symptoms in the HCV transgenic mice were completely blocked by intravenous injection of TNF-α and IL-6 neutralizing antibodies indicated that the progression of chronic hepatitis depended on inflammatory cytokines in serum, rather than the HCV protein levels in hepatocytes. Lymphocytes, macrophages, hepatocytes, and adipocytes each produce TNF-α and IL-6 [30,31], and HCV-infected patients have elevated levels of TNF-α and IL-6 [32,33]. Both cytokines also contribute to the maintenance of hepatosteatosis in mice fed a high-fat diet [34], and production of TNF-α and IL-6 is elevated in obese mice due to the low grade inflammatory response that is caused by lipid accumulation [35]. These findings indicate that both cytokines are responsible for HCV-triggered hepatosteatosis, and anti-cytokine neutralization is a potential treatment for chronic hepatitis if antiviral therapy is not successful.

The reduction of macrophages in number might be due to the induction of apoptosis by vaccinia virus *in vitro* infection as previous reported [36]. To understand the mechanisms responsible for the reduction of the number of macrophage, we performed another experiment to confirm whether the macrophages were infected with vaccinia virus inoculation. However, based on PCR analyses; vaccinia virus DNA was not present in liver tissue that contained macrophages (Figure S7). Furthermore, apoptosis of macrophages was not detected in liver samples (Data not shown). Based on these results, it is unlikely that the reduction in the number of macrophages was due to apoptosis induced by vaccinia virus infection. Although rVV-N25 reduced the number of macrophage, precise mechanism is still unknown. Further examination to elucidate the mechanism is required.

In conclusion, our findings demonstrated that rVV-N25 is a promising candidate for an HCV vaccine therapy. Additionally, the findings of this study indicate that rVV-N25 immunization can be used for prevention of HCV infection and as an antiviral therapy against ongoing HCV infection.

Materials and Methods

Ethics Statement

All animal care and experimental procedures were performed according to the guidelines established by the Tokyo Metropolitan Institute of Medical Science Subcommittee on Laboratory Animal Care; these guidelines conform to the Fundamental Guidelines for Proper Conduct of Animal Experiment and Related Activities in Academic Research Institutions under the jurisdiction of the Ministry of Education, Culture, Sports, Science and Technology, Japan, 2006. All protocols were approved by the Committee on the Ethics of Animal Experiments of the Tokyo Metropolitan Institute of Medical Science (Permit Number: 11–078). All efforts were made to minimize the suffering of the animals.

Animals

R6CN2 HCV cDNA (nt 294–3435) [37] and full genomic HCV cDNA (nt 1–9611) [38,39] were cloned from a blood sample taken from a patient (#R6) with chronic active hepatitis (Text S1). The infectious titer of this blood sample has been previously reported [40]. R6CN2HCV and R6CN5HCV transgenic mice were bred with Mx1-Cre transgenic mice (purchased from Jackson Laboratory) to produce R6CN2HCV-MxCre and R6CN5HCV-MxCre transgenic mice, which were designated CN2-29$^{(+/-)}$/MxCre$^{(+/-)}$ and RzCN5-15$^{(+/-)}$/MxCre$^{(+/-)}$ mice, respectively. Cre expression in the livers of these mice was induced by intraperitoneal injection of polyinosinic acid–polycytidylic acid [poly(I:C)] (GE Healthcare UK Ltd., Buckinghamshire, England); 300 μL of a poly(I:C) solution (1 mg/mL in phosphate-buffered saline [PBS]) was injected three times at 48-h intervals. All animal care and experimental procedures were performed according to the guidelines established by the Tokyo Metropolitan Institute of Medical Science Subcommittee on Laboratory Animal Care.

Histology and Immunohistochemical Staining

Tissue samples were fixed in 4% paraformaldehyde in PBS, embedded in paraffin, sectioned (4-μm thickness), and stained with hematoxylin and eosin (H&E). Staining with periodic acid–Schiff stain, Azan stain, silver, or Oil-red-O was also performed to visualize glycogen degeneration, fibrillization, reticular fiber degeneration, or lipid degeneration, respectively.

For immunohistochemical staining, unfixed frozen liver sections were fixed in 4% paraformaldehyde for 10 min and then incubated with blocking buffer (1% bovine serum albumin in PBS) for 30 min at room temperature. Subsequently, the sections were incubated with biotinylated mouse anti-HCV core mono-

clonal antibody (5E3) for 2 h at room temperature. After being washed with PBS, the sections were incubated with streptavidin–Alexa Fluor 488 (Invitrogen). The nuclei were stained with 4',6-diamidino-2-phenylindole (DAPI). Fluorescence was observed using a confocal laser microscope (Laser scanning microscope 510, Carl Zeiss).

Generation of rVVs

The pBR322-based plasmid vector pBMSF7C contained the ATI/p7.5 hybrid promoter within the hemagglutinin gene region of the vaccinia virus, which was reconstructed from the pSFJ1-10 plasmid and pBM vector [41,42]. Separate full-length cDNAs encoding either the HCV structural protein, nonstructural protein, or all HCV proteins were cloned from HCV R6 strain (genotype 1b) RNA by RT-PCR. Each cDNA was inserted into a separate pBMSF7C vector downstream of the pBMSF7C ATI/p7.5 hybrid promoter; the final designation of each recombinant plasmid was pBMSF7C-CN2, pBMSF7C-N25, or pBMSF-CN5 (Figure 2). They were then transfected into primary rabbit kidney cells infected with LC16m8 (multiplicity of infection = 10). The virus–cell mixture was harvested 24 h after the initial transfection by scrapping; the mixture was then frozen at −80°C until use. The hemagglutinin-negative recombinant viruses were cloned as previously described [42] and named rVV-CN2, rVV-N25, or rVV-CN5. Insertion of the HCV protein genes into the LC16m8 genome was confirmed by direct PCR, and expression of each protein from the recombinant viruses was confirmed by western blot analysis. The titers of rVV-CN2, rVV-N25, and rVV-CN5 were determined using a standard plaque assay and RK13 cells.

Statistical Analysis

Data are shown as mean ± SD. Data were analyzed using the nonparametric Mann–Whitney or Kruskal–Wallis tests or ANOVA as appropriate; GraphPad Prism 5 for Macintosh (GraphPad) was used for all analyses. P values <0.05 were considered statistically significant.

Supporting Information

Figure S1 HAI score of liver samples taken from CN2-29$^{(+/-)}$/MxCre$^{(+/-)}$ mice.
(EPS)

Figure S2 Lipid degeneration in samples of liver taken from CN2-29$^{(+/-)}$/MxCre$^{(+/-)}$ mice.
(EPS)

Figure S3 HCV protein expression after infection of LC16m8, rVV-CN2, rVV-N25, or rVV-CN5 into HepG2 cells.
(EPS)

Figure S4 Effects of treatment with rVV-N25 in RzCN5-15$^{(+/-)}$/MxCre$^{(+/-)}$ mice.
(EPS)

Figure S5 Daily cytokine profiles of the serum from CN2-29$^{(+/-)}$/MxCre$^{(+/-)}$ mice during the week following inoculation with LC16m8, rVV-CN2, rVV-N25, or rVV-CN5.
(EPS)

Figure S6 The immune response following poly(I:C) injection in the acute phase.
(EPS)

Figure S7 Detection of vaccinia virus DNA in the skin, liver, and spleen after inoculation with attenuated vaccinia virus (Lister strain) or highly attenuated vaccinia virus (LC16m8 strain).
(EPS)

Table S1 Incidence of hepatocellular carcinoma in male and female transgenic mice at 360, 480, and 600 days after poly(I:C) injection.
(EPS)

Text S1 Supporting information including material and methods, and references.
(DOCX)

Acknowledgments

We thank Dr. Fukashi Murai for supporting this study. We also thank Dr. Keiji Tanaka for providing the MxCre mice, Dr. Shigeo Koyasu for providing the GK1.5 (anti-CD4) and 53–6.72 (anti-CD8) monoclonal antibodies, and Dr Takashi Tokuhisa for helpful discussions.

Author Contributions

Performed the experiments: SS KK TC Y. Tobita TO FY Y. Tokunaga. Analyzed the data: SS KK TC MK. Contributed reagents/materials/analysis tools: KT-K TW TT MM K. Mizuno YH TH K. Matsushima. Wrote the paper: SS KK MK. Study concept and design: MK.

References

1. Lauer GM, Walker BD (2001) Hepatitis C virus infection. N Engl J Med 345: 41–52.
2. Alter MJ (1995) Epidemiology of hepatitis C in the West. Semin Liver Dis 15: 5–14.
3. Kawamura T, Furusaka A, Koziel MJ, Chung RT, Wang TC, et al. (1997) Transgenic expression of hepatitis C virus structural proteins in the mouse. Hepatology 25: 1014–1021.
4. Moriya K, Fujie H, Shintani Y, Yotsuyanagi H, Tsutsumi T, et al. (1998) The core protein of hepatitis C virus induces hepatocellular carcinoma in transgenic mice. Nat Med 4: 1065–1067.
5. Wakita T, Katsume A, Kato J, Taya C, Yonekawa H, et al. (2000) Possible role of cytotoxic T cells in acute liver injury in hepatitis C virus cDNA transgenic mice mediated by Cre/loxP system. J Med Virol 62: 308–317.
6. Wakita T, Taya C, Katsume A, Kato J, Yonekawa H, et al. (1998) Efficient conditional transgene expression in hepatitis C virus cDNA transgenic mice mediated by the Cre/loxP system. J Biol Chem 273: 9001–9006.
7. Folgori A, Capone S, Ruggeri L, Meola A, Sporeno E, et al. (2006) A T-cell HCV vaccine eliciting effective immunity against heterologous virus challenge in chimpanzees. Nat Med 12: 190–197.
8. Chisari FV, Ferrari C (1995) Hepatitis B virus immunopathology. Springer Semin Immunopathol 17: 261–281.
9. Machida K, Tsukiyama-Kohara K, Seike E, Tone S, Shibasaki F, et al. (2001) Inhibition of cytochrome c release in Fas-mediated signaling pathway in transgenic mice induced to express hepatitis C viral proteins. J Biol Chem 276: 12140–12146.
10. Kuhn R, Schwenk F, Aguet M, Rajewsky K (1995) Inducible gene targeting in mice. Science 269: 1427–1429.
11. Li K, Chen Z, Kato N, Gale M Jr, Lemon SM (2005) Distinct poly(I-C) and virus-activated signaling pathways leading to interferon-beta production in hepatocytes. J Biol Chem 280: 16739–16747.
12. Sugimoto M, Yamanouchi K (1994) Characteristics of an attenuated vaccinia virus strain, LC16m0, and its recombinant virus vaccines. Vaccine 12: 675–681.
13. Youn JW, Hu YW, Tricoche N, Pfahler W, Shata MT, et al. (2008) Evidence for protection against chronic hepatitis C virus infection in chimpanzees by immunization with replicating recombinant vaccinia virus. J Virol 82: 10896–10905.
14. Guidotti LG, Rochford R, Chung J, Shapiro M, Purcell R, et al. (1999) Viral clearance without destruction of infected cells during acute HBV infection. Science 284: 825–829.
15. Burkett MW, Shafer-Weaver KA, Strobl S, Baseler M, Malyguine A (2005) A novel flow cytometric assay for evaluating cell-mediated cytotoxicity. J Immunother 28: 396–402.

16. Pasquinelli C, Shoenberger JM, Chung J, Chang KM, Guidotti LG, et al. (1997) Hepatitis C virus core and E2 protein expression in transgenic mice. Hepatology 25: 719–727.
17. Lerat H, Honda M, Beard MR, Loesch K, Sun J, et al. (2002) Steatosis and liver cancer in transgenic mice expressing the structural and nonstructural proteins of hepatitis C virus. Gastroenterology 122: 352–365.
18. Lang KS, Georgiev P, Recher M, Navarini AA, Bergthaler A, et al. (2006) Immunoprivileged status of the liver is controlled by Toll-like receptor 3 signaling. The Journal of clinical investigation 116: 2456–2463.
19. Jasani B, Navabi H, Adams M (2009) Ampligen: a potential toll-like 3 receptor adjuvant for immunotherapy of cancer. Vaccine 27: 3401–3404.
20. Elmowalid GA, Qiao M, Jeong SH, Borg BB, Baumert TF, et al. (2007) Immunization with hepatitis C virus-like particles results in control of hepatitis C virus infection in chimpanzees. Proc Natl Acad Sci U S A 104: 8427–8432.
21. Satoi J, Murata K, Lechmann M, Manickan E, Zhang Z, et al. (2001) Genetic immunization of wild-type and hepatitis C virus transgenic mice reveals a hierarchy of cellular immune response and tolerance induction against hepatitis C virus structural proteins. J Virol 75: 12121–12127.
22. Crispe IN (2009) The liver as a lymphoid organ. Annu Rev Immunol 27: 147–163.
23. Chisari FV (2005) Unscrambling hepatitis C virus-host interactions. Nature 436: 930–932.
24. Saito T, Sherman GJ, Kurokohchi K, Guo ZP, Donets M, et al. (1997) Plasmid DNA-based immunization for hepatitis C virus structural proteins: immune responses in mice. Gastroenterology 112: 1321–1330.
25. Large MK, Kittlesen DJ, Hahn YS (1999) Suppression of host immune response by the core protein of hepatitis C virus: possible implications for hepatitis C virus persistence. Journal of immunology 162: 931–938.
26. Dustin LB, Rice CM (2007) Flying under the radar: the immunobiology of hepatitis C. Annu Rev Immunol 25: 71–99.
27. Bowie A, Kiss-Toth E, Symons JA, Smith GL, Dower SK, et al. (2000) A46R and A52R from vaccinia virus are antagonists of host IL-1 and toll-like receptor signaling. Proc Natl Acad Sci U S A 97: 10162–10167.
28. Zhu J, Martinez J, Huang X, Yang Y (2007) Innate immunity against vaccinia virus is mediated by TLR2 and requires TLR-independent production of IFN-beta. Blood 109: 619–625.
29. Samuelsson C, Hausmann J, Lauterbach H, Schmidt M, Akira S, et al. (2008) Survival of lethal poxvirus infection in mice depends on TLR9, and therapeutic vaccination provides protection. J Clin Invest 118: 1776–1784.
30. Sheikh MY, Choi J, Qadri I, Friedman JE, Sanyal AJ (2008) Hepatitis C virus infection: molecular pathways to metabolic syndrome. Hepatology 47: 2127–2133.
31. Tilg H, Moschen AR, Kaser A, Pines A, Dotan I (2008) Gut, inflammation and osteoporosis: basic and clinical concepts. Gut 57: 684–694.
32. Malaguarnera M, Di Fazio I, Laurino A, Ferlito L, Romano M, et al. (1997) Serum interleukin 6 concentrations in chronic hepatitis C patients before and after interferon-alpha treatment. Int J Clin Pharmacol Ther 35: 385–388.
33. Larrea E, Garcia N, Qian C, Civeira MP, Prieto J (1996) Tumor necrosis factor alpha gene expression and the response to interferon in chronic hepatitis C. Hepatology 23: 210–217.
34. Park EJ, Lee JH, Yu GY, He G, Ali SR, et al. (2010) Dietary and genetic obesity promote liver inflammation and tumorigenesis by enhancing IL-6 and TNF expression. Cell 140: 197–208.
35. Gregor MF, Hotamisligil GS (2011) Inflammatory mechanisms in obesity. Annu Rev Immunol 29: 415–445.
36. Humlova Z, Vokurka M, Esteban M, Melkova Z (2002) Vaccinia virus induces apoptosis of infected macrophages. The Journal of general virology 83: 2821–2832.
37. Choo QL, Kuo G, Weiner AJ, Overby LR, Bradley DW, et al. (1989) Isolation of a cDNA clone derived from a blood-borne non-A, non-B viral hepatitis genome. Science 244: 359–362.
38. Tsukiyama-Kohara K, Tone S, Maruyama I, Inoue K, Katsume A, et al. (2004) Activation of the CKI-CDK-Rb-E2F pathway in full genome hepatitis C virus-expressing cells. J Biol Chem 279: 14531–14541.
39. Nishimura T, Kohara M, Izumi K, Kasama Y, Hirata Y, et al. (2009) Hepatitis C virus impairs p53 via persistent overexpression of 3beta-hydroxysterol Delta24-reductase. J Biol Chem 284: 36442–36452.
40. Shimizu YK, Purcell RH, Yoshikura H (1993) Correlation between the infectivity of hepatitis C virus in vivo and its infectivity in vitro. Proc Natl Acad Sci U S A 90: 6037–6041.
41. Yasui F, Kai C, Kitabatake M, Inoue S, Yoneda M, et al. (2008) Prior immunization with severe acute respiratory syndrome (SARS)-associated coronavirus (SARS-CoV) nucleocapsid protein causes severe pneumonia in mice infected with SARS-CoV. J Immunol 181: 6337–6348.
42. Kitabatake M, Inoue S, Yasui F, Yokochi S, Arai M, et al. (2007) SARS-CoV spike protein-expressing recombinant vaccinia virus efficiently induces neutralizing antibodies in rabbits pre-immunized with vaccinia virus. Vaccine 25: 630–637.

RESEARCH PAPER

Oncolmmunology 1:5, 581-592; August 2012; © 2012 Landes Bioscience

Cross-priming for antitumor CTL induced by soluble Ag + polyI:C depends on the TICAM-1 pathway in mouse CD11c$^+$/CD8α^+ dendritic cells

Masahiro Azuma, Takashi Ebihara,† Hiroyuki Oshiumi, Misako Matsumoto and Tsukasa Seya*

Department of Microbiology and Immunology; Hokkaido University Graduate School of Medicine; Sapporo, Japan

†Current affiliation: Howard Hughes Medical Institute; Washington University School of Medicine; St. Louis, MO USA

Keywords: cross-presentation, dendritic cell, TLR3, TICAM-1 (TRIF), tumoricidal CTL

Abbreviations: APC, antigen-presenting cells; CTL, cytotoxic T lymphocytes; DAMP, damage-associated molecular pattern; DC, dendritic cells; IFN, interferon; IPS-1, IFNβ promoter stimulator-1; MDA5, melanoma differentiation associated gene 5; Mf, macrophages; NK, natural killer; OVA, ovalbumin; PAMP, pathogen-associated molecular pattern; PRR, pattern-recognition receptors; PV, poliovirus; RIG-I, retinoic acid inducible gene-1; SL8, an OVA tetramer; TICAM-1, Toll-IL-1 receptor homology domain-containing molecule-1; TLR, Toll-like receptor; WT, wild-type

PolyI:C is a nucleotide pattern molecule that induces cross-presentation of foreign Ag in myeloid dendritic cells (DC) and MHC Class I-dependent proliferation of cytotoxic T lymphocytes (CTL). DC (BM or spleen CD8α$^+$) have sensors for dsRNA including polyI:C to signal facilitating cross-presentation. Endosomal TLR3 and cytoplasmic RIG-I/MDA5 are reportedly responsible for polyI:C sensing and presumed to deliver signal for cross-presentation via TICAM-1 (TRIF) and IPS-1 (MAVS, Cardif, VISA) adaptors, respectively. In fact, when tumor-associated Ag (TAA) was simultaneously taken up with polyI:C in DC, the DC cross-primed CTL specific to the TAA in a syngenic mouse model. Here we tested which of the TICAM-1 or IPS-1 pathway participate in cross-presentation of tumor-associated soluble Ag and retardation of tumor growth in the setting with a syngeneic tumor implant system, EG7/C57BL6, and exogenously challenged soluble Ag (EG7 lysate) and polyI:C. When EG7 lysate and polyI:C were subcutaneously injected in tumor-bearing mice, EG7 tumor growth retardation was observed in wild-type and to a lesser extent IPS-1$^{-/-}$ mice, but not TICAM-1$^{-/-}$ mice. IRF-3/7 were essential but IPS-1 and type I IFN were minimally involved in the polyI:C-mediated CTL proliferation. Although both TICAM-1 and IPS-1 contributed to CD86/CD40 upregulation in CD8α$^+$ DC, H2K^b-SL8 tetramer and OT-1 proliferation assays indicated that OVA-recognizing CD8 T cells predominantly proliferated in vivo through TICAM-1 and CD8α$^+$ DC is crucial in ex vivo analysis. Ultimately, tumor regresses > 8 d post polyI:C administration. The results infer that soluble tumor Ag induces tumor growth retardation, i.e., therapeutic potential, if the TICAM-1 signal coincidentally occurs in CD8α$^+$ DC around the tumor.

Introduction

Cytotoxic T lymphocytes (CTL) and natural killer (NK) cells are two major effectors for antitumor cellular immunity. These effectors are driven through activation of dendritic cells (DC) and/or macrophages (Mf), which is mediated by pattern-recognition receptors (PRRs) for the recognition of microbial patterns.[1,2] Antigen (Ag) presentation and upregulation of NK cell-activating ligands are major events induced in DC/Mf in response to PRRs, which link to evoking CTL- and NK-antitumor immunity, respectively. The immune-potentiating function of specific components of the classical adjuvants are largely attributable to the ligand activity of PRRs (CpG DNA/TLR9, polyI:C/TLR3, monophosphoryl lipid (MPL) A/TLR4, Pam2/TLR2, etc.).[3] That is, the DC/Mf competent to drive effectors are generated through PRR signal in inflammatory nest where affected cells and recruited immune cells encounter exogenous or endogenous PRR ligands. Since studying the functional properties of PRRs in tumor immunity is on the way using a variety of possible ligands and cell biological analyses, immune responses reflecting the total adjuvant potential around Ag-presenting cells (APC) in local inflammatory nests are not always elucidated even in mice.

RNA-sensing PRR pathways, including TLR3-TICAM-1, TLR7-MyD88 and RIG-I/MDA5-IPS-1 participate in driving Type I IFN induction and cellular immunity in DC subsets.[1,4,5] Type I IFN and the IFNAR pathway in DC and other cells reportedly evoke and amplify T cell immunity.[5,6] TLR7 resides exclusively in plasmacytoid DC[7] whereas TLR3 mainly exists in

*Correspondence to: Tsukasa Seya; Email: seya-tu@pop.med.hokudai.ac.jp
Submitted: 02/04/12; Revised: 03/02/12; Accepted: 03/02/12
http://dx.doi.org/10.4161/onci.19893

myeloid DC/Mf and epithelial cells.[8] They are localized on the membrane of the endosome and deliver the signal via their adaptors, MyD88 and TICAM-1.[7,8] RIG-I and MDA5 are ubiquitously distributed to a variety of mouse cells and signal the presence of cytoplasmic viral products through IPS-1.[9] Thus, TLR3 and RIG-I/MDA5 are candidates associated with DC maturation to drive effector cells.[10] Indeed, viral dsRNA analog, polyI:C, is a representative ligand for TLR3 and MDA5 and induces polyI:C-mediated DC-NK reciprocal activation.[11,12] These are also true in human DC.[13]

The point of this study is by which pathway antitumor CTL are induced for tumor regression in a mouse tumor-implant model. It has been postulated that DC present exogenous tumor Ag to the MHC Class I-restricted Ag-presentation pathway and proliferate CD8 T cells specific to the extrinsic Ag. When tumor cells provide soluble and insoluble exogenous Ag, this Class I Ag presentation occurs mostly TAP/proteasome-dependent, suggesting the pathway partly sharing with that for endogenous Ag presentation. This DC's ability to deliver exogenous Ag to the pathway for MHC Class I-restricted Ag presentation has been described as cross-presentation.[14] DC cross-presentation leads to the cross-priming and proliferation of Ag-specific CD8 T cells in vivo and in vitro.[14-18] A variety of PAMP[15,16] and intrinsic DAMP[17] as well as other factors including Type I IFN,[5,18] $CD4^+$ T cells[19] and NKT cells[20] augment cross-priming in tumor-bearing mice. However, by what molecular mechanism polyI:C enhances CTL induction in tumor-bearing mice remains largely unsettled.

Here, we made an EG7 tumor-implant mouse system and treated the mice with s.c.-injected ovalbumin (OVA)-containing cell lysates (Ag) and polyI:C. Spleen $CD8\alpha^+$ DC turn CTL-inducible when stimulated with Ag and polyI:C. In either case of s.c., i.p., or i.v. injection of polyI:C, the TLR3/TICAM-1 pathway predominantly participates in $CD8\alpha^+$ DC cross-priming and antitumor CTL induction. Earlier studies using non-tumor models, suggested that both TLR3 and MDA5 appeared to participate in polyI:C-dependent CTL induction.[21] TLR3 is predominantly involved in primary Ag response and Th1 skewing,[22] while MDA5 participates in secondary Ag response.[23] Importance of TLR3 in induction of cross-priming was first suggested by Schulz et al., who used OVA/polyI:C-loaded or virus-infected xenogenic (Vero) cells and mouse DC.[16] Here we demonstrate that the antitumor polyI:C activity is sustained by the TICAM-1 pathway in any route of injection in tumor-implant mice: antitumor CTL responses are mostly abrogated in TICAM-$1^{-/-}$ but not IPS-$1^{-/-}$ mice.

Results

Properties of EG7 tumor with high MHC in tumor-loading mice. The properties of the EG7 line we used are consistent with those reported previously.[24,25] It expressed high MHC Class I (H2-Kb) and no Qa-1b or Rae-1 (**Fig. S1**). The expression levels of these proteins were barely changed before and after implantation of EG7 cells into mice. Cell viability was not affected by in vitro stimulation with polyI:C only (**Fig. S1B**). However, a batch-to-batch difference of cell viability may have affected the rate of tumor growth in each mouse tumor-implant experiment.

$CD8^+$ T cells are responsible for tumor retardation by polyI:C. EG7 cells (2×10^6) were inoculated into the back of C57BL/6 (WT), and the indicated reagents were subcutaneously (s.c.) injected around the EG7 tumor (**Fig. 1A**). Growth retardation of tumor was observed by treatment with polyI:C or polyI:C plus EG7 lysate (**Fig. 1A**). EG7 lysate only had no effect on tumor regression. When $CD8\beta^+$ T cells were depleted before EG7 lysate/polyI:C treatment, polyI:C-mediated tumor growth suppression was cancelled (**Fig. 1A**), suggesting the participation of CD8 T cells in tumor growth suppression. The therapeutic potential of polyI:C appeared to be more reproducible in the presence of EG7 lysate than in the absence, judged from the increases of activated $CD8^+$ T cells (**Fig. 1B**) and cytotoxic activity (**Fig. 1C**) of LN T cells isolated from the mice sacrificed after the last therapy. Yet, the EG7 Ag could be more or less supplied from the implant tumor. $NK1.1^+$ cells did not participate in this EG7 tumor regression in this setting (data not shown).

Since EG7 lysate contains OVA, OVA-specific T cells in draining LN and spleen of the WT mice were counted by tetramer assay after the last therapy (**Fig. S2A and B**). The numbers of tetramer-positive cells were prominently increased in LN and spleen in mice with EG7 lysate and polyI:C. We confirmed the importance of simultaneous administration of Ag plus polyI:C for OVA-specific CTL induction as in **Figure S2C**, where pure Ag (OVA) was used instead of EG7 lysate for immunotherapy. The polyI:C adjuvant function appeared to be more efficient in the mixture of pure Ag than in polyI:C alone. Tumor regression (**Fig. S2C**) and OVA-specific CTL induction (**Fig. S2D**) were clearly observed in this additional experiment. To obtain reproducible data, we employed the EG7 lysate/polyI:C combination therapy as follows.

IFN-inducing pathways are involved in PolyI:C-derived EG7 growth retardation. We next inoculated EG7 cells (2×10^6) into the back of C57BL/6 (WT), TICAM-$1^{-/-}$, IPS-$1^{-/-}$, or TICAM-1/IPS-1 double-deficient (DKO) mice (**Fig. 2**). We s.c. administered EG7 lysate with or without polyI:C around the tumor. The EG7 lysate was the soluble fraction of EG7 which removed insoluble debris by centrifugation. The EG7 lysate contained unprecipitated micro-debris and soluble Ag. No other emulsified reagent was added for immunization. Thus, the adjuvant function of polyI:C per se is reflected in the tumor growth, although polyI:C had to be injected into mice twice a week. Retardation of tumor growth was observed $>$ 8 d after immunization with EG7 lysate + polyI:C in WT mice, though no growth retardation without polyI:C (**Fig. 2A**). The polyI:C-mediated tumor growth suppression was largely abrogated in TICAM-$1^{-/-}$ (**Fig. 2B**) and to a lesser extent in IPS-$1^{-/-}$ mice (**Fig. 2C**), and completely in TICAM-1/IPS-1 DKO mice (**Fig. 2D**). Hence, TICAM-1 plays an important role in inducing polyI:C-mediated tumor growth retardation in the s.c. setting we employed.

CD8 T cell activation induced by the TICAM-1 pathway. CD8 T cell activation in the inguinal LN was tested with polyI:C + EG7 lysate in EG7 tumor-bearing mice using CD69 as

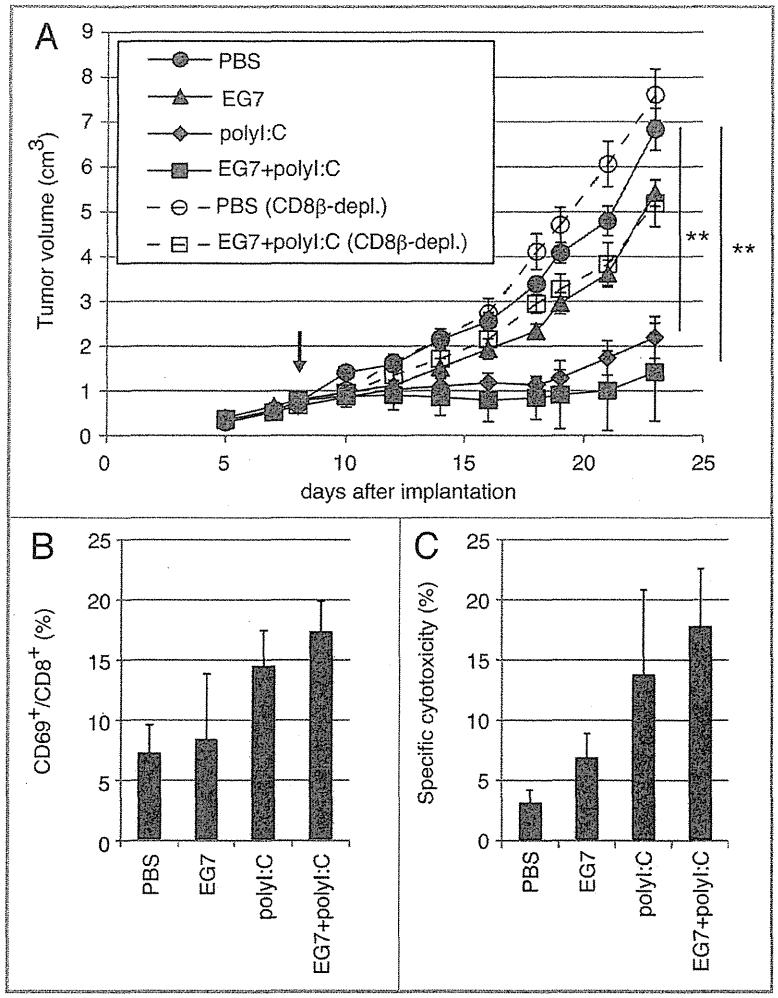

Figure 1. PolyI:C induces CTL-mediated tumor regression. (A) WT mice were challenged with EG7 cells and were treated with PBS (●), EG7 lysates (▲), polyI:C (◆) and EG7 lysates + polyI:C (■). The adjuvant therapy was started at the time indicated by the arrow and the indicated reagents injected twice per week. One of the two PBS groups (○) and one of the two EG7 lysates + polyI:C groups (□) were treated with anti-CD8β ascites in order to deplete $CD8^+$ T cells once a week. Each group had 3–5 mice. (B) Draining inguinal LNs were harvested 24 h after the last treatment and the proportion of CD69-expressing $CD8^+$ cells were counted. (C) LN cells were co-cultured with MMC-treated EG7 cells for 3 d and subjected to ^{51}Cr release assay to evaluate CTL activity. E/T = 50. All error bars used in this figure show ± SEM. Data are representative of two independent experiments. One-way analysis of variance (ANOVA) with Bonferroni's test was performed to analyze statistical significance. **, $p < 0.01$.

an activating marker. Twenty-four hours after the last polyI:C + EG7 sec.c. treatment, cells were harvested from the LN excised (**Fig. 3A**). FACS profiles of total cells from each mouse group are shown in **Fig. S3**. By combination therapy with EG7 lysate and polyI:C, T cells were activated in WT and IPS-$1^{-/-}$ mice, but the proportion of CD8 T cells was not affected by the therapy (**Fig. S4A**). Under the same conditions, T cells were barely activated in TICAM-$1^{-/-}$ mice in response to polyI:C (**Fig. 3A**). The proportion of $CD69^+$ cells are indicated in **Figure 3B**. IL-2 (**Fig. 3C**) and IFNγ (**Fig. S4B**) were highly induced in the WT and IPS-$1^{-/-}$ LN cells, while they were not induced in TICAM-$1^{-/-}$ or DKO cells. IFNγ levels were upregulated only in polyI:C-treated tumor-bearing mice, although the WT > IPS-$1^{-/-}$ profile for IFNγ production was reproducibly observed (**Fig. S4B**).

In vivo proliferation of CD8 T cells judged by tetramer assay and IFNγ induction. We next tested whether i.p. injection of polyI:C plus OVA induces CTL proliferation. PolyI:C and OVA were i.p. injected into mice and the polyI:C-dependent cross-priming of CD8 T cells were examined using the OVA tetramer assay. OVA-specific CD8 T cells were clonally proliferated in WT and IPS-$1^{-/-}$ mice, but not in TICAM-1/IPS-1 DKO and IRF-$3/7^{-/-}$ mice (**Fig. 4A**). Proliferation of OVA-specific CD8 T cells were severely suppressed in TICAM-$1^{-/-}$ mice (**Fig. 4A**), suggesting that polyI:C-mediated cross-priming of CD8 T cells largely depends on the TICAM-1 pathway followed by IRF-3/7 activation in the i.p. route. The results were reproduced in additional experiments using more mice (**Fig. 4B**) and TLR$3^{-/-}$ mice (**Fig. S5A and B**). The polyI:C cytokine response, where IFNα is IPS-1-dependent while IL-12p40 is TICAM-1-dependent, was also confirmed in serum level by polyI:C i.p. injection (**Fig. S5E**). Specific induction of IFNγ (**Fig. 4C**) was also observed in parallel with the results of **Figure 4A**.

Whether or not i.v. injection of polyI:C plus OVA induces Ag-specific CTL and cytotoxicity was next checked. OVA-specific OT-1 proliferation and cytotoxicity (**Fig. 4D and E**) were observed in in vivo analyses of WT and IPS-$1^{-/-}$ CD8 T cells but not of TICAM-$1^{-/-}$, TICAM-1/IPS-1 DKO, and IRF-$3/7^{-/-}$ mice in the i.v. setting.

Since TICAM-1 is the adaptor for TLR3 as well as cytoplasmic helicases,[24] we confirmed the level of cross-priming being decreased in TLR$3^{-/-}$ mice and an expected result was obtained (**Fig. S5A and B**). Furthermore, in IFNAR$^{-/-}$ mice, OVA-specific CTL induction was slightly reduced compared with that in WT mice, but higher than in TICAM-$1^{-/-}$ mice (**Fig. S5C and D**). Hence, in vivo cross-presentation induced by polyI:C mostly depends on the TLR3-TICAM-1 pathway followed by transcriptional regulation by IRF-3/7 in any administration route, and is further promoted by Type I IFN presumably produced by the stromal cells through the IPS-1 pathway.[26]

IPS-1 induces DC maturation but not cross-priming in vivo. Spleen DC maturation by i.v.-injected polyI:C was tested ex vivo using $CD8\alpha^+$ DC and $CD8\alpha^-$ DC isolated from WT or KO mice with no tumor as indicated in **Figure 5A**. The maturation markers CD86 and CD40 were upregulated on both $CD8\alpha^+$ and $CD8\alpha^-$